Structure-property Relations of Permanently Densified Oxide Glass

Svenson, Mouritz Nolsøe

DOI (link to publication from Publisher):
10.5278/vbn.phd.engsci.00176

Publication date:
2016

Document Version
Publisher's PDF, also known as Version of record

STRUCTURE-PROPERTY RELATIONS OF PERMANENTLY DENSIFIED OXIDE GLASSES

BY
MOURITZ NOLSØE SVENSON

DISSERTATION SUBMITTED 2016

AALBORG UNIVERSITY
DENMARK

STRUCTURE-PROPERTY RELATIONS OF PERMANENTLY Ddensified OXIDE GLASSES

by

Mouritz Nolsøe Svenson

AALBORG UNIVERSITY
DENMARK

25/09/2016

.

Dissertation submitted: 25/09/2016

PhD supervisor: Professor MSO, Morten Mattrup Smedskjær,
Aalborg University, Denmark

PhD committee: Associate Professor Donghong Yu (Formand)
Aalborg Universitet, Denmark

Professor, Leena Hupa,
Åbo Akademi University, Finland

Professor Sung Keun Lee
Seoul National University, Republic of Korea

PhD Series: Faculty of Engineering and Science, Aalborg University

ISSN (online): 2246-1248
ISBN (online): 978-87-7112-807-9

Published by:
Aalborg University Press
Skjernvej 4A, 2nd floor
DK – 9220 Aalborg Ø
Phone: +45 99407140
aauf@forlag.aau.dk
forlag.aau.dk

Printed in Denmark by Rosendahls, 2016

ENGLISH SUMMARY

In contrast to the periodic arrangements of crystalline lattices, the structure of glass is characterized by a lack of long range order. Due to this network arrangement, glasses exhibit continuous changes in structure and properties as a function of temperature and pressure, although polyamorphic transitions with discontinuous changes have been observed in few cases. As a result, the structure and properties of glasses are sensitive to the details of their pressure-temperature history (*P*-*T* history). Substantial research efforts have been devoted to the influence of composition and thermal history on the structure and properties of glasses, whereas the influence of pressure history is significantly less understood, and to and to an even smaller extent the combined effects of pressure-temperature variations. The aim of the current thesis is to reveal the influence of combined pressure-temperature treatments on the structure and properties of oxide glasses.

To investigate the bulk properties of glasses, pressure-treated samples of sufficient size are required. These can be obtained at relatively low pressures (even <1 GPa) by simultaneous application of elevated temperature. In the current work, we focus on compression of glasses at their ambient pressure T_g temperature. So far, most studies have focused on pressure-induced structural changes, whereas others have included properties such as diffusivity, density, glass transition behavior, and mechanical properties. The relation between pressure-induced changes in structure and properties is however not well understood. In the present thesis, we investigate pressure-induced changes in structure and a range of properties (e.g., elastic moduli, glass transition behavior, and hardness) of glasses by using nuclear magnetic resonance spectroscopy (NMR), Raman spectroscopy, Brillouin spectroscopy, differential scanning calorimetry (DSC), and Vickers indentation. We also investigate the influence of variations in compression temperature on densification behavior.

Based on relaxation experiments and comparisons between different densification methods, we find changes in different glass properties to depend on specific structural changes invoked by compression at T_g. After compression, a general relation between relative changes in density and elastic moduli is found is found across a variety of glass compositions. Similarly, a general relation between the dissociation energy per volume and the plastic compressibility is found across a wide range of glass compositions.

DANSK RESUME

I modsætning til det periodiske arrangement i krystallinske gitre er strukturen af glas karakteriseret ved manglen på orden over lang skala. På grund af dette netværks arrangement udviser glasser kontinuerlige ændringer i struktur og egenskaber som funktion af tryk og temperatur, selvom polyamorfe faseovergange med diskontinuerlige ændringer er blevet observeret i få tilfælde. Som følge af dette er strukturen og egenskaberne af glas følsomme overfor ændringer i deres tryk-temperatur historie. Betydelig mængder af forskning er blevet udført for at forstå indflydelsen af komposition og termisk historie på strukturen of egenskaberne af glas, hvorimod indflydelsen af tryk historie er væsentligt mindre forstået, og i endnu mindre grad den kombinerede effekt af tryk-temperatur variationer. Formålet med nærværende tese er at udrede indflydelsen af kombineret tryk-temperatur behandlinger på struktur og egenskaber af oxid glasser.

For at undersøge egenskaberne af glas er trykbehandlede prøve emner af tilstrækkelig størrelse nødvendige. Disse kan produceres ved relativt lave tryk (<1GPa) ved samtidig anvendelse af øget temperatur. I nærværende projekt har vi fokuseret på tryk af glas ved glasovergang temperaturen, målt ved atmosfærisk tryk. Indtil nu har de fleste studier fokuseret på tryk-inducerede ændringer i struktur, hvorimod andre har inkluderet egenskaber så som diffusion, massefylde, opførsel af glasovergangen og mekaniske egenskaber. Relationen mellem tryk-inducerede ændringer i struktur og egenskaber er dog ikke forstået I dybden. I nærværende tese undersøger vi tryk-inducerede ændringer i struktur og en række egenskaber (f.eks. elastiske moduli, opførsel af glasovergangen og hårdhed) af oxid glasser ved brug af kernemagnetisk resonans spektroskopi (NMR), Raman spektroskopi, Brillouin spektroskopi, differentiel kalorimetri og indentation. Vi undersøger også indflydelsen af variationer i temperaturen anvendt under tryk på densifikations opførslen.

Baseret på relaksations eksperimenter og sammenligninger mellem forskellige densifikations metoder finder vi at ændringer i forskellige egenskaber af glas afhænger af specifikke strukturelle ændringer induceret efter tryk ved T_g. Vi finder at der gælder en general relation for de relative ændringer i densitet og elastiske moduli efter tryk. Vi finder også en general relation mellem energien for bindingsspaltning pr. volume og den plastiske kompressibilitet, på tværs af en lang række glas kompositioner.

PREFACE AND ACKNOWLEDGEMENTS

This thesis has been submitted for assessment in partial fulfillment of the Ph.D. degree. The thesis is based on the submitted or published scientific papers which are listed in Section 1.3. The Ph.D. study was carried out from October 1st 2013 to October 1st 2016. The work was primarily conducted at the Section of Chemistry at Aalborg University, with an external stay at Rensselaer Polytechnic Institute (New York, USA) for ½ month. The study was financed by a license from the Danish Council for Independent Research under Sapere Aude: DFF-Starting Grant (1335-00051A).

I would like to thank my supervisor Morten Mattrup Smedskjær for dedicated guidance and support throughout this Ph.D. project. He has met suggestions and initiatives with a positive approach, creating an environment rich in learning, creativity and productivity. I would further like to thank our collaborators at Corning Inc.: John Mauro and Randall Youngman. John has contributed in scientific discussions, manuscript writing, and arrangements for my stay at Corning. He has been very positive and helpful with all my enquiries, and always found time to reply e-mails with a minimum of waiting time. Randall has performed dedicated NMR analysis, fundamental to the work of this Ph.D. project. He has furthermore been involved with scientific discussions, writing of manuscripts and taken time to guide me through my visit at Corning. You have both been inspirational and excellent collaborators!

I would like to thank our collaborators in Warsaw, Poland: Michal Bockowski and Sylwester Rzoska. Both have been of fundamental necessity for the execution of this Ph.D. project, by performing compression experiments and participating in scientific discussions and manuscript reviews.

I would like to thank our collaborators at RPI: Liping Huang and Michael Guerette. Both were of great help in technical instructions for operation of the diamond anvil cell, along with the use of Brillouin spectroscopy. A special thank goes to Michael, who spend long days working with me in the lab and made the stay a fun and efficient learning experience.

I would like to thank our collaborator at Aalborg University: Lars Rosgaard, who has been very helpful in operation and support with Raman spectroscopy of central importance to this project.

I would further like to thank our collaborator in Madrid, Spain: Fransisco Muñoz, who was of great help in our study on oxynitride glasses, with expertise within the field, performing NMR analysis and contribution in manuscript preparation.

Finally I would like to thank my co-workers at the department of chemistry at Aalborg University: Rasmus Guldbæk, Kacper Januchta, Søren Sejer Donau, Laura Paraschiv, Rene Thomsen, Kim Thomsen, Rasmus Rosenlund, Martin Bonderup Østergaard Bonderup, Tobias Kjær Bechgaard, Hao Liu and Chao Zhou, for good company, support with technical and scientific issues, for valuable scientific discussions and your contributions in making the chemistry department a fun and pleasant working environment.

TABLE OF CONTENTS

CHAPTER 1. INTRODUCTION

Glass finds wide applications in modern society, from components in electronic systems and energy technology, to building materials and window panes [1]. The production of man-made glass reaches back thousands of years, with the very first applications being based on its decorative value, optical properties and practical use for containers. These applications were based on a soda-lime-silica composition [2], presumably due to the availability and glass forming ability of these elements. Early challenges in the application of glass lay in the optical quality and the resistance towards moisture attack. However, with minor chemical refinements, these properties were optimized, and soda-lime-silica based glasses still constitute the majority of commercial glasses today, typically used for containers and flat glasses. Despite of the thousand years old production of glass, the study of glass structure and properties only really started to develop as a field of science (i.e. glass science) about 100 years ago [2]. With increasing technological development, a demand for improved glasses followed, leading to major advances in glass quality and properties in Germany in the late 19th century [2]. For example, a demand for glasses with high thermal shock resistance in the late 19th century led to the commercial introduction of borosilicate glasses.

Since then, the development of new glasses has accelerated, resulting in a variety of glass compositions ranging in use from batteries and insulation to bioactive materials and lightguide fibers [1]. The latter being a notable example, which formed the basis of an entire new industry [2]. Today, glass has become an important material in modern society, ideally suited for a range of applications due to a unique combination of optical transparency, ease of forming and good mechanical properties. However, with increasing demands for high performance glasses, further scientific development is required.

In the past 100+ years of glass science, studies on glass properties have mainly focused on the effects of composition and/or temperature [3][4][5]. These are important parameters, manifested in the effect of e.g. composition on viscosity [4], which is vital in the processing of glass. The increased understanding of the influence of temperature and composition on glass properties has also led to composition-property models [6] and temperature-property [7] models, with the earliest composition-property model dating as far back as 1894 [3]. Such models have previously been successfully applied in the development of glasses, with more recent examples including ab initio computer simulations [8].

Much effort has also been devoted to the study of glass structure [9]. The basic concept of an amorphous structure of glass was introduced in the 1930´s, based on oxide glasses [10]. In general, the local structure of glass (i.e. coordination polyhedra) closely resemble the atomic arrangements found in crystals [11], but

lacks the periodic arrangements of crystal lattices. Due to this amorphous nature, a complete structural description cannot be obtained similarly for glasses as for crystals by diffraction methods. Therefore, a variety of structural probes have been applied in the attempt to unravel the structure of glass. These include: Nuclear Magnetic Resonance Spectroscopy (NMR), neutron diffraction, small- and wide angle X-ray scattering (SAXS/WAXS), X-ray Absorption Fine Structure (XAFS) and molecular dynamics simulations [9][10]. This has led to an enhanced understanding of glass structure for a variety of glass systems, and based on this understanding, models on structure-property relations have also been suggested [12].

With a developed understanding of glass structure and properties as a function of composition and temperature, studies on the effect of other variables have also commenced. In the 1960´s, the response of glass to pressure in the rigid [13] and non-rigid state [14], along with subsequent heat treatment (relaxation) [15], was studied by McKenzie. It was found that by performing compression at room temperature, a lower threshold pressure had to be exceeded for permanent densification (i.e. densification is elastic at low pressure and temperature). With higher pressure or temperature, a gradual densification occurred as a function of the pressure and temperature applied. This gradual densification stands in contrast to the polymorphic transitions seen in minerals, where pressure-induced changes between crystal structures cause abrupt changes in density. Glasses generally have a higher free volume than their crystalline counterparts and therefore have a lower density. E.g. v-B_2O_3 has a density of 1.81 g/cm^3 [16][17], which is ~41 % lower than its crystalline counterpart (2.56 g/cm^3) [18], and SiO_2 has a density of 2.2 g/cm^3, which is ~20 % lower than its crystalline counterpart (2.65 g/cm^3) [19]. Significant densification of glass is possible, as seen for example in the case of SiO_2, where pressure-induced densification of up to 25% has been reported from compression at 8 GPa at 1100 °C [20].

A growing number of studies on compressed glasses have described some of the structural changes occurring during pressure-densification [21][22][23]. Compression studies can enhance our understanding of glass structure, which is relevant for the design of glasses with optimized mechanical properties. E.g. compressed glasses have been found to display an increased hardness [24][22]. The mechanical properties of glass are of utmost importance for application purposes and compression may serve as a novel route for optimization of glass properties. A detailed understanding of the pressure-induced changes in structure and properties, and structure-property relations, however remains lacking.

1.1. BACKGROUND AND CHALLENGES

Due to an increased use of glass in technological applications, there is an increased demand for advanced glasses with tailored properties. Especially the damage resistance of glass is currently receiving wide attention. The damage resistance of

glass is highly relevant across various application, from cockpit windows and energy technology, to touch screens in personal electronic devices [25]. The recent development in damage resistant touch screens is a testimony of the current progress within the field.

An important mechanical property of glass is the hardness, which is a measure of the resistance towards elasto-plastic deformation, such as surface scratching. This property has become increasingly important with the advent of touch screen devices, since scratches compromise the transparency and lower the strength of display covers. Hardness was one of the first mechanical properties studied in glass science, with the first indentation test in glass being performed in the late 1940´s [26]. Since then, indentation testing of glasses has proven an easy method for evaluating the hardness of glass. The hardness measured by this method is a product of three different deformation modes; elastic deformation, volume conservative shear flow and densification [27][28]. Densification during indentation is the dominant deformation mode in inorganic oxide glasses, and a deformation mode unique to glasses [29]. Therefore, it is of fundamental interest to understand the densification behavior of glass in relation to its mechanical properties.

Furthermore, the density and hardness of glass can be increased through compression, making compression of glass a potential method for property optimization [15][32][26][28]. Hereby, compression may be of industrial relevance. Little is however known about the structural mechanisms governing the pressure-induced changes in properties. Pressure-induced structure and property changes have previously been studied at ambient temperature [23] and elevated temperature [33][34][35] within the geological community. These studies have mainly been conducted to understand thermodynamics and transport properties under mantle conditions in the Earth's interior. Such studies have demonstrated marked changes in glass structure and properties after compression [36][37]. The pressure-induced structural changes are fundamentally different than the changes obtained by variation of thermal history alone, and therefore compression also offers an additional means for fundamental studies on structure-property relations. Studies of compressed glasses is therefore of both scientific and practical interest.

1.2. OBJECTIVES

The overall objective of this Ph.D. thesis is to study the pressure-induced changes in structure and properties of glasses. The focus will mainly be on the pressure induced structure-property modifications resulting from compression at T_g, at pressures up to 1 GPa. However, additional variations of treatment, such as varying compression temperature and combined compression and chemical strengthening will also be applied, to explore further processing regimes of compressed glasses.

The specific objectives of the Ph.D. thesis are summarized as follows:

1. Clarify the relation between chemical composition and densification behavior of inorganic oxide glasses
2. Understand the relations between pressure induced changes in structure-density-mechanical properties
3. Investigate the relaxation behavior of structure and properties in compressed glasses
4. Investigate the combined effects of compression and ion exchange on the mechanical properties of glass
5. Investigate the influence of compression temperature on the densification behavior of oxide glass

1.3. THESIS CONTENT

This thesis is organized as a plurality, including an introductory overview of glass structure and densification methods, followed by eight journal papers (either published or submitted for publication). An overview of the journal papers is listed below:

I. M.N. Svenson, M. Guerette, L. Huang, M.M. Smedskjær, "Raman spectroscopy study of pressure-induced structural changes in sodium borate glass", *Journal of Non-Crystalline Solids,* **443**, 130–135 (2016)

II. M.N. Svenson, T.K. Bechgaard, S. D. Fuglsang, R.H. Pedersen, A.Ø. Tjell, M.B. Østergaard, R. E. Youngman, J. C. Mauro, S. J. Rzoska, M. Bockowski, M.M. Smedskjaer, Composition-Structure-Property Relations of Compressed Borosilicate Glasses, *Physical Review Applied*, **2**, 024006 (2014)

III. M.N. Svenson, L.M. Thirion, R.E. Youngman, J.C. Mauro, S.J. Rzoska, M. Bockowski, M.M. Smedskjaer, Pressure-Induced Changes in Interdiffusivity and Compressive Stress in Chemically Strengthened Glass, *ACS Applied Materials and Interfaces*, **6**, 10436−10444 (2014)

IV. M.N. Svenson, L.M. Thirion, R.E. Youngman, J.C. Mauro, M. Bauchy, S.J. Rzoska, M. Bockowski, M.M. Smedskjaer, Effects of Thermal and Pressure histories on the chemical strengthening of sodium aluminosilicate glass, *Frontiers in Materials*, **3**, 14, (2016)

V. M.N. Svenson. R.E. Youngman, Y. Yue, S.J. Rzoska, M. Bockowski, L. R. Jensen, M.M. Smedskjaer, Volume and Structure Relaxation in Compressed Sodium Borate Glass, *Physical Chemistry Chemical Physics* (submitted).

VI. M.N. Svenson, G. L. Paraschiv, F. Muñoz, Y. Yue, S.J. Rzoska, M. Bockowski, L.R. Jensen, M.M. Smedskjaer, Pressure-Induced Structural Transformations in Phosphorus Oxynitride Glasses, *Journal of Non-Crystalline Solids*, **52**, 153-160 (2016)

VII. M.N Svenson. J.C. Mauro, S.J. Rzoska, M. Bockowski, M.M. Smedskjær, Accessing Forbidden Glass Regimes through High-Pressure Sub-T_g Annealing, *In preparation*, 2016

VIII. M.N Svenson. M. Guerette, L. Huang, N. Lönnroth, J.C. Mauro, S.J. Rzoska, M. Bockowski, M.M. Smedskjaer, Universal behavior of changes in elastic moduli of hot compressed oxide glasses, *Chemical Physics Letters*, **651**, 88-91 (2016)

CHAPTER 2. STRUCTURE, PROPERTIES AND DENSIFICATION METHODS OF GLASS

Different glass compositions show network arrangements and macroscopic properties inherent to the glass chemistry. When studying the densification of glass, it is therefore relevant to consider a variety of glass compositions in order to understand the overall densification behavior of glass. Density driven changes in properties are derived from structural changes, and therefore a structural understanding of glass is necessary. The structural arrangements of glasses vary significantly with composition, and structural knowledge encompassing different compositional regimes is therefore needed. However, structural changes as a function of density also depend on the processing method [20]. It is therefore also relevant to consider the influence of different densification methods. For example, glasses with identical chemical composition and density, but differences in elastic moduli and relaxation behavior can be formed, depending on the processing method, as recently reported for SiO_2 glass densified equally trough hot- or cold compression [20]. The processing route (e.g. P-T history) is therefore also of importance in order to understand the final glass state. As an introductory overview, the structure of relevant glass compositions, properties and densification methods is therefore described in the following,

2.1. GLASS TRANSITION BEHAVIOR

When cooling a glass-forming melt, continuous relaxation of structure and properties occurs. This is illustrated in Figure 2-1, which shows the volume and enthalpy of a glass forming liquid during cooling. As shown in the figure, the liquid can be cooled below its melting point, into a supercooled liquid, which upon further cooling can experience a glass transition. The glassy state and the glass transition is widely recognized as one of “the deepest and most interesting unsolved problem in solid state theory”, as opined by Anderson [38]. The change from liquid into glass is in principle possible for all compositions, if the cooling rate is high enough to avoid crystallization.

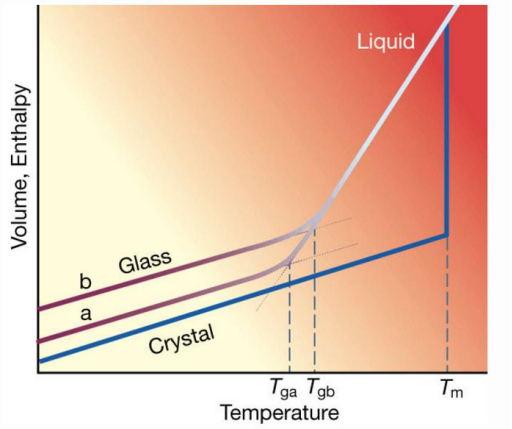

Figure 2-1. Volume or enthalpy of a glass forming melt as a function of temperature. With a sufficiently high cooling rate, the liquid can be cooled below its melting point into the supercooled liquid. Depending on the cooling rate, the supercooled liquid experiences a glass transition at T_{gb} (fast cooling) or T_{ga} (slow cooling), which in turn affects the volume and enthalpy of the final glass. Figure adopted from [39].

The temperature range which separates the supercooled liquid from a glass is called the glass transition region, and it is accompanied by non-monotonic changes in properties such as volume, enthalpy and heat capacity [39]. Structurally, this temperature range can be considered the point at which the kinetic barriers exceed the structural relaxation time. It is however important to emphasize that the glass transition does not cause complete structural arrest, as continued relaxation can occur below this temperature range [40]. ·

It is convenient to describe the temperature which separates a supercooled liquid from a glass by a single temperature. In Figure 2-1 this is denoted by T_{ga} and T_{gb}. In this thesis, these points will be termed the glass transition onset temperatures. As seen from the figure, the same glass composition can have different onset temperatures. Due to the time dependence of structural relaxation, a high cooling rate produces a glass with a high onset temperature, whereas a low cooling rate produces a glass with a low onset temperature. This in turn affects the density and properties of the final glass. To have a standardized term for the transition temperature between the supercooled liquid and glass, independent of kinetic factors (i.e. cooling rate), the temperature at which the viscosity equals 10^{12} Pa s has been suggested (T_g). This is also how the term T_g is also applied in the current thesis. This temperature can conveniently be obtained from DSC measurements, by the onset temperature when a heating rate of 10 K/min has been applied, after the glass experienced a cooling rate of 10 K/min [41][42]. The temperature at which the liquid freezed into a glass is in named the fictive temperature. Different methods for

determination of this temperature has been suggested [43]. In the case where the glass is cooled and re-heated with the same rate (e.g. 2 K/min), the onset temperature has been found to corresponds to the fictive temperature [44]. The onset temperature is found from the intersection point between the glass C_p and the tangent to the steepest point on the up-slope of the glass transition (see Figure 2-2).

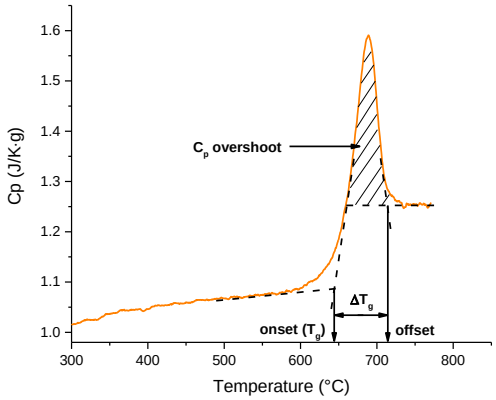

Figure 2-2. DSC scan of the glass transition region with illustration of relevant parameters for characterization of the glass transition behavior. If the glass experienced a cooling rate of 10 K/min, followed by a heating rate of 10 K/min during the DSC scan, the onset temperature denotes T_g.

Similarly, the offset temperature can be found from the intersection point between the tangent of the supercooled liquid and the tangent of the steepest point on the down slope of the glass transition (see Figure 2-2). The temperature interval between these two temperature points is denoted ΔT_g. The ΔT_g obtained when applying a heating rate of 10 K/min, after having cooled the glass with 10 K/min, has been found to scale with fragility of the glass (i.e. the rate of viscosity change as a function of temperature) [4][45].

Compression has been found to cause changes in the glass transition behavior [22], and to quantify these changes, definition of further parameters is necessary. E.g. compression had been found to increase the enthalpy overshoot [1] [22] [44]. The enthalpy overshoot is illustrated as the hatched area in Figure 2-2. This area is also known to increase with sub-T_g annealing (structural relaxation) [48]. Interestingly, the C_p overshoot does not decrease during mechanical stretching, which instead causes a sub-T_g exotherm, similar to that seen in hyperquenched glasses [49]. The C_p overshoot is caused by an endotherm process. Hereby it represents energy that has been released from the system during prior relaxation, and has to be added to the system for the glass to convert into a supercooled liquid. The metric of the system

(measured by DSC) is energy stored in chemical bonds. This indicates that the enthalpy overshoot represent energy released from chemical bonds during structural relaxation (e.g. slow cooling), which is returned during heating, allowing for the glass-supercooled liquid transition. Based on sub-T_g annealing of hyperquenched glass fibers, changes in the C_p overshoot has also been suggested to represent primary relaxation, i.e. relaxation of the backbone structure of the glass network [50].

2.2. STRUCTURE OF GLASS

Since the introduction of Zachariasens random network theory in 1932 [51], the theory on glass structure has developed significantly. A fundamental concept for the structure of glass is the different roles occupied by different elements in the glass. These include; network formers, intermediates and modifiers. According to this theory, certain elements (e.g. Si, B and Ge) form tightly constrained coordination polyhedra, defining the backbone structure of the glass (network formers). Other elements (e.g. Na, Ca) occupy the interstices within the glass network and hereby modify the structure (modifiers). The last category (intermediates) consists of elements (e.g. Al) which can act as network formers or network modifiers, depending on the glass structure and chemistry.

An increased development in the theory of glass structure arrived with the advent of new analytical methods. In 1985, Greaves applied Extended X-ray Absorption Fine Structure (EXAFS) to study the modifier environment in glasses. Based on his results, he suggested a modification of the random network theory (modified random network theory). According to this theory, modifiers do not distribute randomly within the glass network, but gather in channel like structures.

Using further analytical methods, more composition specific structural features of glass networks have also been elucidated. E.g. The use of fluorescence excitation and molecular dynamics simulations has proved the presence of boroxol rings in B_2O_3 glass [52][53]. Due to the variation in glass structure as a function of chemistry, theory on glass structure within different compositional regimes is required. In the following, a brief summary on glass structure within compositions relevant for the present thesis is described.

2.2.1. SILICATE GLASSES

SiO_2 is a classic glass former and the structure and properties of vitreous SiO_2 has been widely studied [20]. The structure of vitreous SiO_2 has also recently been observed by ADF-STEM [54] (cf. Figure 2-3), showing remarkable resemblance with the original random network theory by Zachariasen [51]. The basic building block of the network is a silicon atom connected to four oxygen atoms in a tetrahedral configuration. Tetrahedra are further connected with each other by each

corner, with a Si-O-Si angle varying around 144° [55]. Upon the addition of network modifiers, oxygens starts changing role from forming bridging oxygens (BOs), connecting two network formers, into forming non-bridging oxygens (NBOs), connecting a network former with a network modifier. The number of bridging oxygens on a tetrahedron are usually described by the Q^n notation, where n is the number of bridging oxygens. SiO_2 glass hereby consists entirely of Q^4 species, and when adding modifiers, the number of BOs on each tetrahedron starts to decrease from 4 to 3 (i.e. from Q^4 to Q^3) etc.

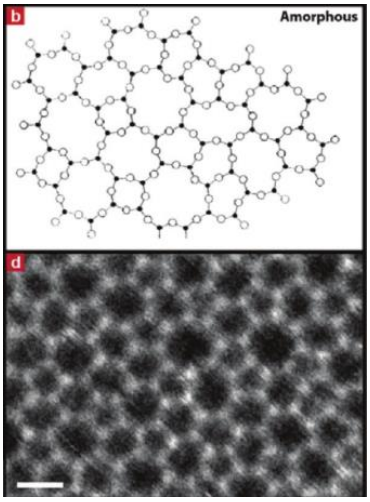

Figure 2-3. Top: Illustration of Zachariasen´s random network theory for SiO_2 glass. Bottom: ADF-STEM image of two dimensional SiO_2 glass. Remarkable similarity of the network arrangements is seen between the illustrations. Figure reproduced from [54].

2.2.2. ALUMINOSILICATE GLASSES

Aluminum is an intermediate and can therefore act both as a network former and modifier, depending on the glass structure and chemistry. Aluminum can enter the glass network in Al^{IV}, Al^{V} or Al^{VI} configuration. The valency of aluminum (Al^{3+}) requires charge balancing to enable the Al^{IV} configuration. When adding modifiers to binary SiO_2-Al_2O_3 glass, the modifiers charge balance Al^{V} and Al^{VI} into Al^{IV} configuration. However, if Al_2O_3 is added in excess of the network modifiers, Al^{V} and Al^{VI} is formed [56].

2.2.3. BORATE GLASSES

Vitreous B_2O_3 consists of boron atoms connected with three oxygen atoms in a planar trigonal configuration [52]. These planar trigonal BO_3 units are connected in

well-defined intermediate range structures (boroxol rings), interconnected by loose BO_3 units. There is now general agreement that v-B_2O_3 is comprised of approximately 80% boron in boroxol rings [57][58].

Upon addition of modifiers, non-monotonic changes in a range of properties have been observed for borate glasses [59], referred to as the "boron anomaly". The boron anomaly occurs when modifiers cause a coordination change from BO_3 to BO_4, with the latter being charge balanced by the modifier cation [60]. The concentration of BO_4 increases steadily in the glass until a given alkali concentration has been reached. Then alkali addition has a reverse impact on BO_4 concentration, as further alkali addition causes formation of NBOs.

2.2.4. BOROSILICATE GLASSES

Adding silica into vitreous B_2O_3 causes intermixing of silica and boron polyhedra, resulting in Si-O-B linkages. A high degree of mixing has been found [61], approximating random mixing [62]. Upon introduction of network modifiers, NBOs and BO_4 can be formed. It has been found that especially non-ring BO_3 are converted into BO_4 upon the addition of modifiers [63].

2.2.5. PHOSPHATE GLASSES

Vitreous P_2O_5 consists of PO_4 tetrahedra, with one distinct π-bonded (P=O) oxygen on each tetrahedron, termed terminal oxygen (TO). The number of non-bridging oxygens (NBO) on the tetrahedra can be described using the Q^n notation, where n is the number of BO atoms per PO_4 tetrahedra. Hereby, pure P_2O_5 glass is built up of Q^3 tetrahedra only. Upon the addition of modifiers, non-bridging oxygens (NBO) are formed. When reaching an equal amount of modifers and phosphorous (e.g. $NaPO_3$), the structure ideally consists only of chains (Q^2 tetrahedra), interconnected by ionic bonds between the NBOs and the modifier cations [64].

2.2.6. OXYNITRIDE GLASSES

Oxynitride glasses are formed by introduction of nitrogen into the anionic network of oxide glasses. This can be achieved by inclusion of nitrogen-containing raw materials in the melting batch. By further application of pressure-quenching, pure nitride glasses have also been formed [65][66]. Alternatively, nitridation can be performed by treatment of the oxide glass melt in an anhydrous ammonia atmosphere (NH_3) at elevated temperature [67][68]. This causes partial substitution of nitrogen into the glass network, in either two-fold (N_d) or three-fold (N_t) coordination [69]. The introduction of nitrogen increases the network cross-linking and causes densification [70] and increased hardness and T_g [71]. For the methaphoshate composition (e.g. $NaPO_3$), the introduction of nitrogen causes a stepwise conversion of PO_4 into PO_3N, and PO_3N into PO_2N_2 [72].

2.3. MECHANICAL PROPERTIES OF GLASSES

Optimizing the mechanical properties of glass is detrimental for future applications [25]. Ideally, knowledge on the structure of glass should enable modelling of mechanical properties, but the development of damage resistant glasses is hampered by an incomplete understanding of structure and structure-property relations. These issues can be illustrated by a short summary on the key predictive models for elastic moduli and glass hardness.

The most successful predictive models for the elastic moduli of glass require knowledge on the atomic packing density and the molar dissociation energies of the constituent oxides [73]. This has led to successful predictions for silicate and aluminosilicate glasses, while showing limited success for phosphate-, borate-, germinate- and aluminate glasses [74][75]. It has been noted that this model is only reliable for glasses with compositions close to their crystalline counterparts, for which the ionic radii are accurately known. In the case of oxide glasses, neither the atomic volumes nor the bonding energies are often known with sufficient accuracy [75], i.e. further understanding of glass structure is required for successful predictive models. Predictive models for the hardness of glass have also been suggested, based on elastic moduli [76] and network topology [77][12]. However, these models have only been successfully applied within limited compositional regimes. A deeper understanding of glass structure and its relation to mechanical properties is therefore required for future property optimization.

The hardness of glass is the result of three different deformation modes: Elastic deformation, plastic densification and volume conservative shear flow. The hardness measured from an indentation imprint is the plastic deformation resulting from densification and shear flow. The quantities of each process can be determined by Yoshida's method [78]. Following this protocol, the glass to indentation followed by 2 hrs annealing at 0.9 T_g, which causes relaxation of the densified part of the indent. By use of, e.g., atomic force microscopy (AFM), the volumes of the indent before and after annealing can be quantified. From the difference in volume, the volumetric changes resulting from densification and shear flow can be quantified.

We have previously applied this method to compressed glasses and found that compression increases the hardness of glass primarily by increasing the resistance towards densification (see Figure 2-4).

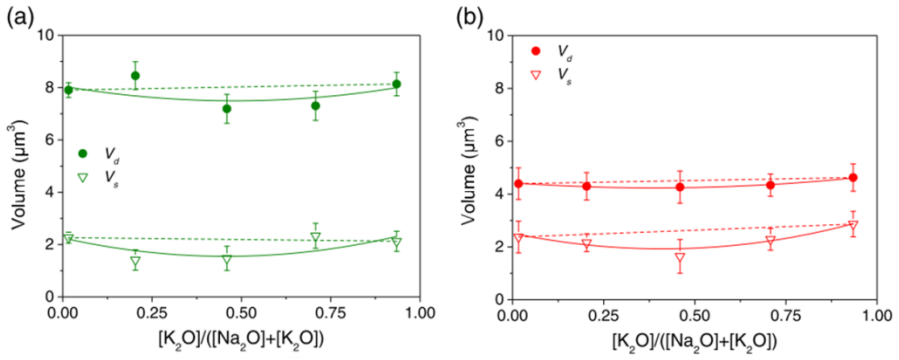

Figure 2-4. Volumes of densification and shear flow in indentation imprints of aluminosilicate glasses with constant modifier content, but varying $[K_2O]/([K_2O]+[Na_2O])$, as quantified by Yoshidas method [78]. (a) uncompressed glasses. (b) glasses compressed at 1 GPa at their respective ambient pressure T_g values. Figure adopted and modified from [31].

This could indicate that the hardness increases merely due to the bulk density increase of the sample after hot compression. However, relaxation experiments of compressed glasses have shown a decoupling between the relaxation times of hardness and density during ambient pressure annealing. This indicates that the pressure-induced hardness increase cannot solely be attributed to the pressure-induced bulk density increase.

2.4. DENSIFICATION METHODS

Glasses can be densified by various methods. Traditionally, glasses are produced by cooling of a melt with sufficient cooling rate to avoid crystallization. Depending on the cooling rate, the glass structure can experience varying degrees of relaxation during cooling from the super-cooled liquid through the glass transition region, resulting in glasses of different densities and fictive temperatures. Glasses can also be produced by other methods, and the choice of production method influences the structure and density of the glass.
The density of glasses can also be modified after production (post-treatment), by e.g. compression. This can yield high-density glasses, but the temperature applied during compression influences the changes in properties as a function of density, making the distinction between different compression methods important.

2.4.1. SUB-T_g ANNEALING

Structural relaxation of the glass network modifies the density and hardness of glasses [5]. For normal glasses, this results in a network compaction, whereas it causes a network expansion for anomalous glasses (e.g. SiO_2). Structural relaxation

is not defined solely by the cooling rate applied during quenching, since continued structural relaxation can occur below the glass transition region. Hereby, isothermal annealing below the glass transition temperature (sub-T_g annealing) can modify the structure, density and hardness of glass [2][37]. To obtain this effect, it is important that annealing is performed at a temperature below the initial fictive temperature of the glass. The density variations that can be obtained by variations in cooling rate or by sub-T_g annealing are however limited to a few percent, and other methods for studies on structure-density-property relations are therefore desired.

2.4.2. COLD COMPRESSION

Compression at room temperature is conventionally referred to as cold compression, in contrast to compression at elevated temperature (hot compression). Cold compression can be performed by compression in diamond anvil cells (DACs) where high pressures (> 10 GPa) can easily be reached. Various types of designs have been developed for diamond anvil cells, but all are based on the same core principle, illustrated in Figure 2-5. However, by using this method, only small sample specimens can be processed (μm^2 range). High pressures can also be reached with other instrumental designs, such as multianvil or piston cylinder devices, producing samples typically in the mm^2 range. Coupled with *in situ* structural characterization (e.g., vibrational spectroscopy, inelastic X-ray scattering, X-ray and neutron diffraction), these types of compression experiments have been applied to explore key structural transformations occurring during densification within a variety of glass systems [80][81][82][21][83][84][85][86].

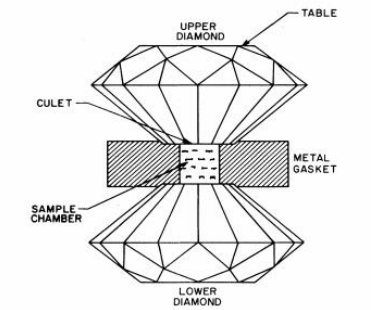

Figure 2-5. The basic principle of the DAC consists of a sample being placed between the flat parallel faces of two opposed diamond anvils. Pressure is generated when a force pushes the two opposed anvils together. Figure adopted from [87].

However, the limitations in specimen dimensions suitable for these types of compression methods are problematic in relation to analysis of macroscopic properties (e.g., hardness and durability), and for potential industrial applications, where larger sample specimens would typically be required. The structural analysis which can be obtained by these methods is however relevant in terms of understanding fundamental structural changes during densification of glass.

2.4.3. HOT COMPRESSION

Compression can be performed at elevated temperature, causing permanent densification at significantly lower pressures than required in cold compression [88][89][90][91][20]. At room temperature, most pressure-induced structural changes remain reversible upon decompression, at pressures below 5–10 GPa [92]. However, by compressing glasses at their glass transition temperature (T_g), a linear increase in density is obtained as a function of pressure, at pressures below 1 GPa [24][22]. Furthermore, hot compression also enables the preparation of bulk sample specimens (cm^2 range), allowing for more comprehensive mechanical testing (e.g. Vickers indentation). However, while there have been numerous studies of glass structure as a function of pressure at room temperature, there are much fewer examples of simultaneous pressure and temperature treatment on glass structure.

Previous studies have found that permanent densification can be obtained below 1 GPa by compression at temperatures above ~0.7 T_g [93][30]. The temperature at which a glass or glass forming melt is compressed is determining for the structure and properties of the resulting glass [20]. A range of studies have been conducted on glasses quenched from melts under pressure [38][45][95][96]. This has provided rich structural information, often on chemical systems relevant for earth sciences [33][34][35][36][37]. During compression at elevated temperature, a sample is kept under the targeted pressure-temperature conditions for a time above the estimated relaxation time. Afterwards, the sample is cooled and then decompressed. One problem encountered with this type of compression scheme is however that the pressure inside the pressure chamber is usually temperature dependent. This can cause a transient pressure drop during cooling. If pressure drops before, or while, the cooling melt is undergoing a glass transition, relaxation times are still short enough for structural relaxation at the transient pressure. Compression at temperatures above T_g, has therefore been found to result in samples with lower density than compression at T_g [96].

When compressing glasses at T_g, the transient pressure drop during cooling is low, within the temperature regime where structural relaxation can occur on an experimental time scale (i.e. >0.7 T_g). Using the example in Figure 2-7, the transient pressure drop is ~10%. It has previously been found that compression at temperatures around T_g resulted in very similar densities [93], so no significant relaxation is expected from this pressure drop. This type of compression

experiments have not been as widely studied as pressure-quenching, but has recently gained attention [25][26][48]. By performing compression at T_g, fewer problems with structural relaxation occurs because of transient pressure drops during cooling. Furthermore, by performing compression at T_g, glasses are compressed at constant viscosity (i.e. 10^{-12} Pa sec). This allows for comparison of pressure induced changes inherent to the chemical compositions, rather than factors influenced by differences in viscosity at the given compression temperature, e.g. if compression was performed at constant temperature rather than constant viscosity. We note that the T_g value of glasses can change as a function of pressure, but the changes are expected to be small within this pressure regime [97][98]. In our studies we have focused mainly on compression at the ambient pressure glass transition temperature (T_g) of the glasses.

Our hot compression experiments were conducted at the Institute of High Pressure Physics in Warsaw, Poland. The glasses were isostatically compressed inside a vertically positioned nitrogen gas pressure chamber, with an internal diameter of 6 cm. Inside the gas pressure chamber was placed a multizone cylindrical graphite furnace. PtRh6%–PtRh30% thermocouples were used to monitor the temperature during the experiments, arranged along the furnace and coupled with an input power control electronic system. The pressure was monitored by manganin gauges, positioned in the low temperature zone of the pressure chamber. The pressure and temperature was controlled with an accuracy of 1 MPa and 0.1 K, respectively. Typically, a few glass samples were placed inside an Al_2O_3 crucible during the experiment, as illustrated in Figure 2-6.

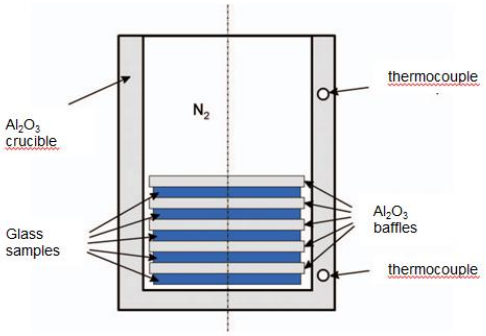

Figure 2-6. Illustration of the gas pressure chamber applied in our hot compression experiments. Samples were stacked in a Al_2O_3 crucible, separated by Al_2O_3 baffles. Nitrogen gas was used as the compression medium. Figure adopted from [30].

When performing experiments, pressure was increased up to a point below the final targeted pressure. Then a constant heating rate of 600 K/h was applied up to the

glass transition temperature, causing an increase in pressure up to the final targeted pressure (see Figure 2-7).

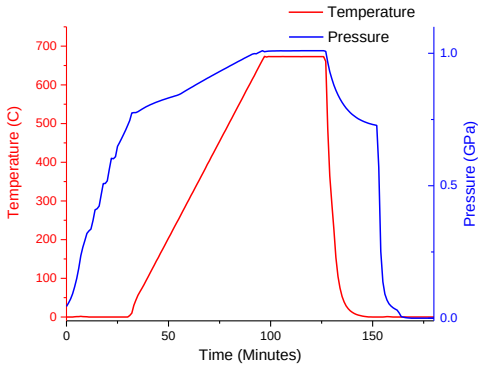

Figure 2-7. Pressure-Temperature profile of a representative hot compression experiment. Pressure inside the pressure-chamber depends on temperature, so the applied pressure was achieved in combination with design of the temperature scheme.

The system was kept at the final pressure at T_g for 30 min, followed by cooling down to room temperature, at a constant rate of 60 K/min. A small pressure drop occurred during cooling, and after cooling, further decompression followed with a rate of 30 MPa/min. It should be noted that nitrogen was used as the compression medium, since its permeability in silicate glasses is low, in contrast to e.g., helium [99].

The current work has focused primarily on compression at the ambient pressure T_g values of glass at pressure up to 1 GPa. Under these conditions, a linear increase in density and properties has been found after hot compression, as a function of the pressure applied, for various glass compositions [19][22][100]. This linear dependence on pressure allows for the definition of a term that states the resistance towards densification of a given glass composition, when compressed under these conditions. This term in named the plastic compressibility:

$$\beta = \frac{\Delta\rho}{\rho_0 P}$$

Where $\Delta\rho$ is the pressure-induced density increase, ρ_0 is the density of the uncompressed glass and P is the pressure applied. This parameter allows for convenient comparison of densification and property changes as a function of composition.

Though the pressure-annealing scheme described in Figure 2-7 was applied for the majority of our pressure experiments [72], [100]–[104], we also applied a specialized pressure-annealing scheme for one study on the effects of *in situ* sub-T_g annealing [105]. In this experiment, we first conducted a conventional hot compression step (as described above). However, for some samples, the hot compression step was not followed by regular cooling and decompression, but instead the temperature was lowered to 0.9 T_g, while pressure was kept constant at 1 GPa (see Figure 2-8). Then samples were kept under these conditions for 2 Hrs or 24 Hrs, followed by cooling and decompression.

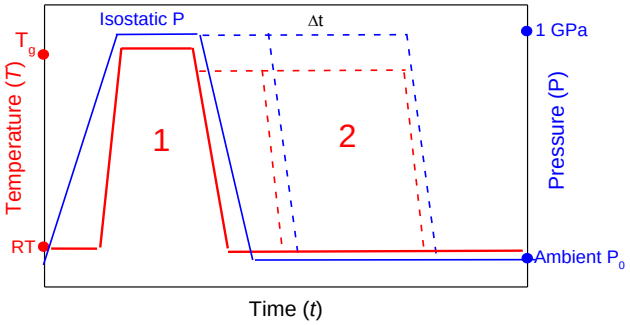

Figure 2-8. Temperature pressure profile including a hot compression step (step 1, solid lines) and and in situ sub-T_g annealing step (step 2, dashed lines).

2.5. RELAXATION

Relaxation of glass forming liquids (i.e., relaxation in the equilibrium state) has been widely studied [106]. However, non-equilibrium relaxation (i.e. relaxation at temperatures below T_g) has received much less attention, due to the exceedingly long timescales involved with relaxation at these temperatures. Various models have been suggested to describe non-equilibrium relaxation of glasses [107][40], but experimental validation of the models is complicated by the relaxation timescales involved, and the fact that non-equilbrium relaxation depends both on the temperature applied and the thermal history of the glass [50].

Relaxation of compressed glasses has not been widely studied [47]. Relaxation can be performed by various annealing protocols. In the current thesis, relaxation has been performed by isothermal annealing at ambient pressure. This can provide interesting information on the pressure-induced structure and property changes [15], but also help to evaluate the stability of compressed glasses for application purposes.

Previously, the elastic moduli of SiO_2 glasses densified equally through hot- or cold compression has was investigated during relaxation [20]. This showed fundamentally different relaxation behaviors of glasses of the same composition and density, but densified by different methods. In addition, recent relaxation experiments have shown a pressure-induced increase BO_4 concentration of a borate glass to remain constant during subsequent density relaxation [22].

Relaxation experiments can also be applied to obtain a deeper understanding of pressure-induced changes in mechanical properties. Compression has previously been found to increase the hardness of glass linearly as a function of pressure [24][22]. By application of Yoshida's method on hot compressed aluminosilicate glasses, it has been found that the pressure induced hardness increase is caused by an increased resistance towards densification [31] (as described in section 2.3). The same mechanism has been found to increase the hardness of pristine glasses after sub-T_g annealing (i.e. increasing resistance towards densification) [79]. The increased resistance towards densification during indentation of hot compressed glasses cannot solely be attributed to the increased bulk density. This is inferred from relaxation experiments, showing that hardness relaxes faster than density [22][101] (see Figure 2-9). This indicates that hardness and density are mutually independent. This in turn indicates that the pressure induced hardness increase is caused by a strengthening of the glass network, but further understanding of the structural origin is required.

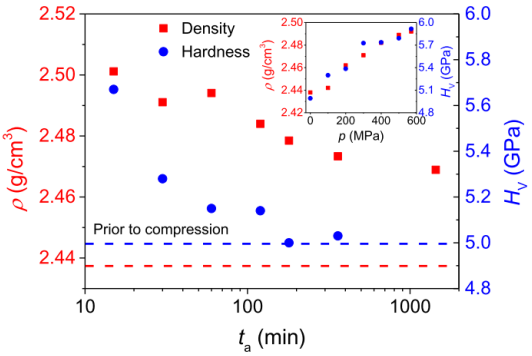

Figure 2-9. Changes in density and hardness during ambient pressure annealing (0.9 T_g) of a hot compressed borate glass. Inset: Density and hardness as a function of pressure after hot compression. Figure adopted from [22].

It is of convenience to define a relaxation function that describes the changes in properties during relaxation as a function of relaxation time. This can be described as follows:

$$M_{\rho}(t_a) = \frac{\rho(t_a) - \rho(\infty)}{\rho(0) - \rho(\infty)}$$

Where $M_{\rho}(t_a)$ varies between 1 and 0 and gives the fraction of the property relaxed at time t_a . In the above equation density is inserted as an example, with $\rho(0)$, $\rho(t_a)$ and $\rho(\infty)$ being the density before annealing, at the given annealing time step, and density of the uncompressed sample after infinite annealing time, respectively. The equation can be similarly applied for other properties (e.g. hardness). As an approximation to the value obtained after infinite annealing time, we have used the value obtained after prolonged annealing (e.g. > 10 000 min) of an uncompressed sample.

Experimental data normalized through the relaxation function can be fitted with the Kohlrausch stretched exponential function [108]:

$$M_{\rho}(t_a) = \exp\left[-\frac{t_a}{\tau}^{\beta}\right]$$

This again provides the fraction of the property relaxed at a given annealing time step (t_a). The variable τ is the characteristic relaxation time for the decay and $0 < \beta \leq 1$ is the dimensionless stretching exponent. It has previously been suggested that β assumes universal values, with $\beta = 3/5$ corresponding to relaxation processes involving both short- and long range rearrangements, whereas $\beta = 3/7$ corresponds to relaxation dominated by long range rearrangements [109].

CHAPTER 3. INFLUENCE OF COMPRESSION TEMPERATURE ON DENSIFICATION BEHAVIOR

Only few comparative studies on the structural changes occurring during hot and cold compression have been performed [20][110][111]. The structural differences between glasses recovered from hot- and cold compression are therefore not well understood. An improved understanding of these differences might, however, enable the prediction of structural changes occurring during hot compression, based on results from cold compression of analogous systems. This could in turn aid in the development of glasses recovered from hot compression with tailored properties, since studies on cold compressed glasses are far more numerous.

By performing compression at elevated temperatures (e.g. T_g), permanent densification of glass can be achieved at pressures significantly lower than by compression at room temperature. At room temperature, there is a lower threshold pressure (typically around 5-10 GPa [92]) for permanent densification of glasses. For hot compressed glasses, permanent densification has been found at pressures down to 0.1 GPa [24].

It has previously been found that temperatures of ~0.7 T_g are necessary for permanent densification at 1 GPa, for a borosilicate glass [93] and an aluminosilicate glass [30]. The onset temperature for permanent densification within this pressure regime may provide further understanding on the densification mechanisms operating during hot compression. However, only few studies have systematically investigated the relation between temperature, pressure and structure in this temperature range [112][93].

3.1. DENSIFICATION AT DIFFERENT TEMPERATURES

To evaluate the impact of the compression temperature on structure and properties, we begin by considering the effect on density. We compressed a commercial aluminosilicate glass at 1 GPa at various temperatures [104][105]. The resulting densities of the samples are shown in Figure 3-1.

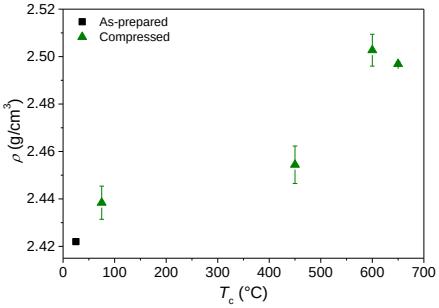

Figure 3-1. Density of an aluminosilicate glass after compression at 1 GPa, plotted as a function of the compression temperature (T_g=650 °C). Compression duration was identical for all glasses (i.e. 0.5 Hrs). Figure adopted and modified from [102].

Only limited densification was obtained by compression below 100 °C. When compression temperature was around 0.7 T_g (450 °C), a slightly increased densification was observed. When compressing at higher temperatures, significantly increased densification was obtained, with the maximum densification remaining approximately constant at temperatures near T_g. This is similar to previous findings for a borosilicate glass [93]. ,

We also studied the structural changes resulting from variation of compression temperatures, using ^{23}Na and ^{27}Al MQMAS NMR. The results are shown in Figure 3-2. A non-linear shift to higher resonance frequency is seen for the ^{23}Na MAS peak, with increasing pressure. ^{27}Al MQMAS NMR was only performed on three samples, but the ^{27}Al δ_{CS} shows the same trend as the ^{23}Na MAS shift. Usually linear changes in structure are seen as function of density when glasses are compressed at T_g, e.g. boron [22][95] or aluminum coordination [113]. Similarly, linear changes in hardness are also usually observed [24][22]. The non-linear ^{23}Na MAS shift to higher frequency with density may indicate differences in the densification mechanisms as a function of compression temperature, but no direct comparison with literature results was possible for glasses compressed at T_g. Included in the plot is also a pristine glass densified by ambient pressure sub-T_g annealing. Sub-T_g annealing caused a shift for both the ^{23}Na MAS NMR peak and the ^{27}Al δ_{CS} in the opposite direction as hot compression. This indicates that compression and sub-T_g annealing densifies glasses through fundamentally different structural mechanisms.

This aligns with recent molecular dynamics simulations, where it was that found compression and sub-T_g annealing impact different parts of the glass network [114].

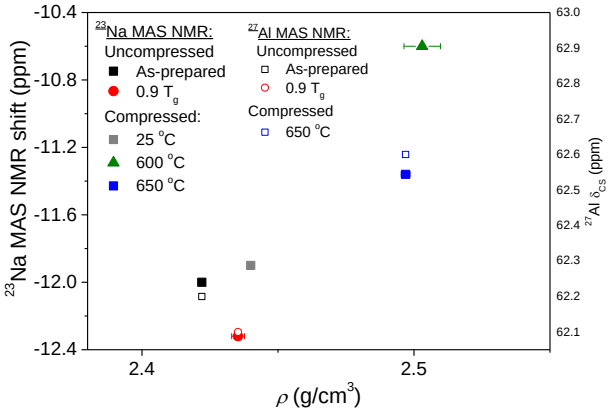

Figure 3-2. ^{23}Na MAS NMR shift and ^{27}Al isotropic chemical shift for an aluminosilicate glass compressed at 1 GPa at various temperatures (t_a=0.5 Hrs). Included is also a non-compressed sample annealed at 0.9 T_g for 168 Hrs. Figure modified and adopted from [103].

3.2. HOT AND COLD COMPRESSION OF A SODIUM BORATE GLASS

To further investigate the differences and similarities between hot- and cold compressed glasses, we studied a sodium borate glass *in situ* during cold compression and *ex situ* after hot compression, using Raman spectroscopy [104]. In the following, a description of the structural changes occurring during hot- and cold compression is provided.

Borate glasses are interesting model systems for studies on pressure induced structural changes, since they display significant changes in both short- and medium range order upon compression. This include changes in coordination number of boron (B^{III} to B^{IV}) and superstructural units (e.g. boroxol rings) [115][116]. For vitreous B_2O_3, a polyamorphic phase transition has also been suggested to occur during decompression [82]. However, only limited high-pressure studies on alkali borate glasses have been conducted [80]. We studied the pressure induced structural changes in a sodium borate glass at pressures up to ~9 GP, using a diamond anvil cell (DAC) combined with *in situ* micro-Raman spectroscopy [104]. The pressure induced changes in the Raman spectra are shown in Figure 3-3.

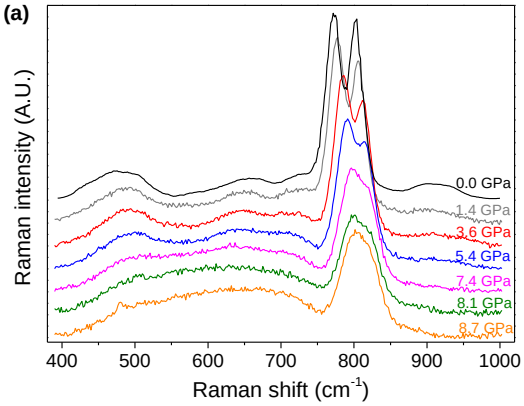

Figure 3-3. Raman spectra of the sodium borate glass during compression up to ~9 GPa, after baseline subtraction and area normalization [117]. Spectra are vertically offset for presentation. Figure adopted from [110].

The two sharp peaks at 770 cm^{-1} and 805 cm^{-1} represent symmetric breathing vibration of triborate and/or tetraborate rings [118][119], and symmetric breathing vibration of boroxol rings [57][120][53], respectively. From the figure, a decrease in the ring structures is seen with increasing pressure, along with an increase in the 650 cm^{-1} peak (assigned to loose BO_3 [121]). The pressure-induced decrease in Raman peaks representing ring structures (770 cm^{-1} and 805 cm^{-1}), combined with the increase in the Raman peak representing loose BO_3 (650 cm^{-1}), indicates a conversion of ring BO_3 into non-ring BO_3 during compression. The sodium borate glass is structurally analogous to v-B_2O_3 and is therefore expected to behave similarly under pressure. For v-B_2O_3, it has previously been found that a breakage of boroxol rings occur during cold compression, based on neutron diffraction [17] and Raman spectroscopy data [115]. Furthermore, a similar breakage of boroxol rings has also been found after hot compression of v-B_2O_3, based on Raman spectroscopy [122], ^{11}B 3QMAS NMR spectroscopy [116], ^{11}B NMR spectroscopy [94], and X-ray diffraction data [94]. In contrast, a reaction scheme involving the stacking of boroxol rings rather than dissolution of the rings, during cold compression of v-B_2O_3, has recently been suggested based on oxygen K-edge spectra [21]. Much less structural data is available for compressed alkali borate glasses, and based on our Raman spectra, we suggest a conversion of rings into non-rings as the most likely scenario under compression.

The same glass composition was also studied after hot compression, and a comparison between the Raman spectra of the hot- and cold compressed samples can be seen in Figure 3-4. It can be seen that the same qualitative changes are observed during cold compression and after hot compression, indicating similar structural changes. However, the Raman spectra shown for the cold compressed glass was measured at 1.4 GPa, i.e. within the elastic regime of densification. This

indicates that the same structural changes can occur elastically during cold compression and in-elastically after hot compression. This, in turn, indicates that these structural changes do not govern density, and that other structural changes may additionally occur during hot- and cold compression, which are not monitored by Raman spectroscopy.

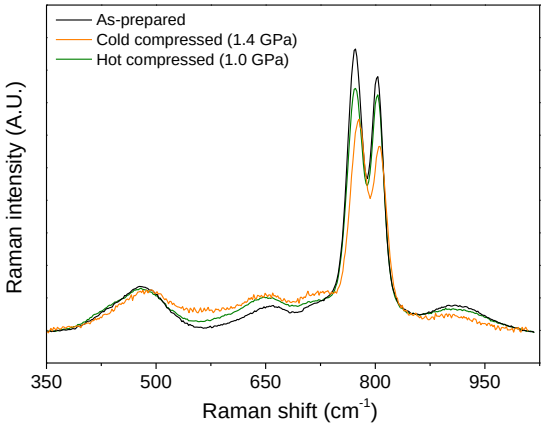

Figure 3-4. Raman spectra of a sodium borate glass *in situ* during cold compression, and *ex situ* after hot compression, compared with the Raman spectra of the as-prepared glass. Figure adopted from [110]

Previous studies comparing the structural changes occurring from hot- and cold compression, using other structural probes, however found fundamental structural differences. A recent ^{11}B MAS NMR experiment probed the MAS shift of a borosilicate glass *in situ* during cold compression and *ex situ* after hot compression [111]. Here it was found that hot compression caused a shift to lower frequency, whereas cold compression caused a shift to higher frequency. This indicates fundamentally different structural changes occurring during hot and cold compression. A recent comparative study on SiO_2 glasses densified equally through hot- and cold compression also showed that the hot compressed sample was more homogenous in structure than the cold compressed sample, and that the two samples showed different relaxation behaviors during ambient pressure annealing [20].

Analogous to these findings, differences in the structural changes resulting from hot- and cold compression may also apply to the investigated sodium borate glass, which are however better monitored by other structural techniques.

3.3. SUMMARY

When densification is obtained by compression at different temperatures, a non-linear change in the ^{23}Na MAS resonance frequency is seen as a function of density. This is in contrast to the linear changes in hardness [24][22] and boron [22][95] and aluminum [113] coordination, usually observed for glasses compressed at T_g. The non-linear change in the ^{23}Na MAS shift may indicate temperature-dependent densification mechanisms. However, no direct comparison with literature results on ^{23}Na MAS NMR shifts was possible. It was also demonstrated from changes in ^{23}Na MAS NMR shifts and ^{27}Al δ_{CS} that densification by ambient pressure sub-T_g annealing and hot compression cause fundamentally different structural changes. This aligns with recent molecular dynamics simulations, showing different types of structural changes resulting from hot compression and ambient pressure sub-T_g annealing [114]

Comparison of the Raman spectra of a sodium borate glass, measured *in situ* during cold compression and *ex situ* after hot compression, showed no qualitative differences in structural changes. Due to the same structural changes being observed after hot compression (permanent densification) and during elastic densification (cold compression <~5 GPa), it is inferred that the densification mechanism cannot be monitored by Raman spectroscopy.

CHAPTER 4. STRUCTURE OF HOT COMPRESSED GLASSES

Continuous structural changes in hot compressed glasses have previously been found as a function of density. Only in few cases have abrupt changes in density and structure been reported in compressed glasses (i.e. polyamorphism) [82][123]. Mechanisms for pressure-induced structural changes have been suggested [124], but the relation between pressure-induced changes in structure and density is not well understood. The structural changes resulting from hot compression have previously been studied by NMR [17][72][80][125][113][126][127][128], x-ray [94] and neutron [17] diffraction, molecular dynamics simulations [5][25] and Raman spectroscopy [20]. In general, an increase in coordination number of network formers is found after compression [18][73][81][126][127][128], along with a compaction of modifier sites [22][95][125][113], and changes in medium range order [20][8][18][20][25]. From the variety of pressure-induced structural changes, it has not yet been possible to unambiguously identify the structural basis for densification.

4.1. SHORT RANGE ORDER

The short range order of glass is usually defined by the first coordination sphere of the given element. This includes changes in coordination number of network forming species and changes in network modifier environments. Increased coordination of network formers has previously been reported in hot compressed glasses of various compositions. This includes an increased coordination of boron (B^{III} to B^{IV}) [22][112], silicon (Si^{IV} to Si^{V} or Si^{VI}) [22][126][127][129] and aluminum (Al^{IV} to A^{lV} or Al^{VI}) [128]. It has also been found that pressure-induced coordination increases are promoted by the presence of NBOs in the pristine glass [95][124][127][130][131]. This has been suggested to occur by a mechanism converting modifiers from a charge modifying role into a charge balancing role [124]. However, minor changes in coordination numbers have also been found in hot compressed glasses with low NBO content ($NaAlSi_3O_8$) [37][36]. Using MAS NMR, we have studied the pressure induced changes in modifier and network former environments after hot compression at 1 GPa at T_g for a borosilicate [101], aluminosilicate [102][103], sodium borate [104] and a series of sodium phospho-oxynitride glasses [72]. In the following, the observed pressure induced changes are described.

4.1.1. MODIFIER ENVIRONMENT

Pressure-induced changes in modifier environments have previously been studied *in situ* during cold compression using diffraction techniques [132], and *ex situ* after hot compression using NMR [95][125][22][113]. Changes in ^{23}Na environment of compressed glasses are relatively easy to study using ^{23}Na MAS NMR. The ^{23}Na resonance frequency has previously been found to shift to higher frequency after hot compression [95][125][22][113].

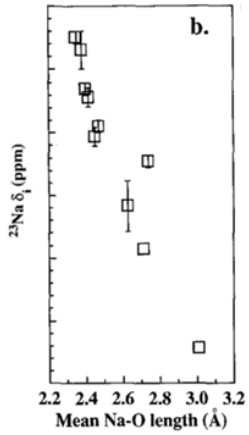

Figure 4-1. Relation between mean Na-O bond length and ^{23}Na isotropic chemical shift, based on anhydrous silicate and aluminosilicate crystals. Figure modified and adopted from Ref. [133].

In anhydrous crystalline silicates and aluminosilicates, an approximately linear relation between ^{23}Na δ_{CS} and Na-O bond lengths has previously been found, as shown in Figure 4-1. In the original paper showing this relation, a formula for determination of bond lengths was not derived [133]. However, in a latter study on the relation between ^{23}Na δ_{CS} and Na-O bond lengths in borate and germanate crystals, this data was fitted with a linear regression, in addition to fits for data on borate and germanate crystals. This provided simple formulas for calculation of bond lengths in silicate, aluminosilicate, borate and germanate glasses, based on the ^{23}Na δ_{CS} shift [134]. The relations are shown in Table 1. Based on these relations, the pressure induced volume changes of the ^{23}Na site in an aluminosilicate glass has been estimated [95]. Here it was found that compaction of the modifier site scaled with overall densification of the sample. The quantification was however based solely on pressure induced changes in the ^{23}Na MAS NMR shift. It was argued that at high magnetic fields, the ^{23}Na MAS NMR peak is controlled mainly by distributions in isotropic chemical shift, and to a lesser extent by second order quadropolar broadening. Hereby, the changes in Na-O bond length after

compression should be possible to evaluate directly from the changes in the ^{23}Na MAS NMR shift, instead of the isotropic chemical shift.

Table 1. Linear fit parameters from the relation between Na-O bond length (Å) and the ^{23}Na δ_{CS} shift (ppm), showing the slope, intercept, R value of the fit and the number of data points the fit was based on. Table reproduced from [134].

Composition	Slope	Intercept	R	Number of data points
Silicates	-67 (6)	179 (16)	0.96	13
Germanates	-47 (25)	130 (68)	0.88	3
Borates	-144 (38)	366 (96)	0.91	5
Carbonates	-66 (21)	159 (52)	0.87	6

We performed ^{23}Na MAS NMR measurements on a hot compressed borosilicate glass [101], aluminosilicate glass [102][103], and sodium borate glasses [104]. In all cases, the ^{23}Na MAS NMR shift was found to move to higher frequency after compression, consistent with literature results [95][125][22][113]. Using ^{23}Na MQMAS NMR, the quadropolar coupling constant and the chemical shift of ^{23}Na can be calculated based on the center of gravity in the MAS dimension and the isotropic dimensions (see appendix A). Using the relations listed in Table 1, we find the volume compaction of the ^{23}Na site in the aluminosilicate glass to be 3.46% after compression at T_g and 1 GPa, which is close to the density change of the bulk sample (~3%). However, when applying the relation for borates (see Table 1) to the sodium borate glass, we find volume compaction of the ^{23}Na site (0.48%) to be much smaller than the density increase of the sample (5.6%). It should be noted that the relation between Na-O bond length and isotropic chemical shift in borates is more uncertain, since fewer data points were available for the linear regression (see Table 1). It should further be noted that if we used ^{23}Na MAS shift instead of ^{23}Na isotropic chemical shift, values for compaction of the ^{23}Na sites much were found much lower than the bulk density change for both the aluminosilicate and the sodium borate glasses

4.1.2. COORDINATION CHANGES OF NETWORK FORMERS

We performed ^{11}B MAS NMR on a sodium borosilicate glass [101] and a sodium borate glass [104]. After compression at 1 GPa, the boron concentration found in fourfold coordination increased from 20.6% to 21.3% for the sodium borate glass, and from 70% to 77% for the borosilicate glass. This is an increase in BO_4 concentration of ~10% in each case, despite of the borate- and borosilicate glasses having widely different plastic compressibility (0.056 and 0.029, respectively). This is similar to a previous finding for a borosilicate glass [93].

We also studied pressure induced changes in aluminum speciation in a commercial aluminosilicate glass [102][103]. In the pristine glass, all ^{27}Al was fourfold coordinated. When compressing the glass at 600 °C at 1 GPa, an increase in Al^V from 0% to 1.7% was found. However, when compressing the sample at higher temperature (T_g=652 °C) at 1 GPa, no increase in Al^V was found. This might be caused by a pressure drop during cooling (as described in section 2.4.3). It has previously been found for aluminosilicate glasses that compression at temperatures above T_g resulted in lower densities and average aluminum coordination than compression at T_g [96]. This was explained by a transient pressure drop during cooling from above T_g, down through the glass transition region. It should however be noted that the coordination changes involved are very small.

Finally, we performed ^{31}P MAS NMR on a $NaPO_3$ glass compressed at 1 GPa at T_g [72]. After compression, only a small shift to lower resonance frequency was found, i.e. no speciation change.

4.1.3. SPECIATION CHANGES IN OXYNITRIDE GLASSES

To study the influence of anion substitution on the densification behavior of glass, we conducted compression experiments on a series of $NaPO_{3-3/2X}N_X$ glasses with N/P ratio varying between 0 and 0.37 [72]. Using ^{31}P MAS NMR, we found a decrease in the fraction of PO_4 units and an increase in the fraction of nitrided species (PO_3N and PO_2N_2 units) after compression at T_g at 1 Gpa. This indicates either an increased average coordination of nitrogen, or increased nitrogen content in the samples, after hot compression. Both scenarios are considered unlikely, based on the following reasons:

1. The $NaPO_4$ base glass did not show presence of nitride species after compression and compression in pure a N_2 atmosphere is known to cause no, or very limited, nitridation [71].
2. Changes in coordination numbers of nitrogen can be monitored by Raman bands located at ~630-640 cm^{-1} (three-fold nitrogen) and ~810-815 cm^{-1} (two-fold nitrogen). These Raman bands did not show changes in intensity after compression.

We therefore suggest an alternative explanation in the following.

Deconvolution of ^{31}P MAS NMR spectra for $NaPO_{3-3/2X}N_X$ glasses requires a minimum of three components, which are assigned to PO_4, PO_3N, and PO_2N_2 tetrahedra, respectively [135]. An increase in the PO_3N peak was seen after compression. However, this peak overlaps with the Q^1 peak (~-9 ppm) and the discrimination between these units is therefore challenging. If the pressure-induced increase in this peak is considered a result of Q^1 formation, the NMR results can be explained without nitridation or coordination changes of nitrogen after compression. We therefore suggest the pressure reactions illustrated in Figure 4-2. These two reactions involve the exchange of a NBO-Na group with a nitrogen atom between two structural units, and can explain conversions between Q_2 and Q_1 units (reaction a), as well as conversions between PO_2N_2 and a PO_3N units (reaction b). From mass balance considerations of these reactions, the quantities of structural units in the compressed glasses can be calculated. Table 2 shows the structural units determined experimentally (NMR) and from mass balance calculations. The suggested pressure reactions (Figure 4-2) do not cause any changes in the quantities of Q^2 and PO_2N_2, i.e. quantities for these structural units are identical for experimental and calculated results.

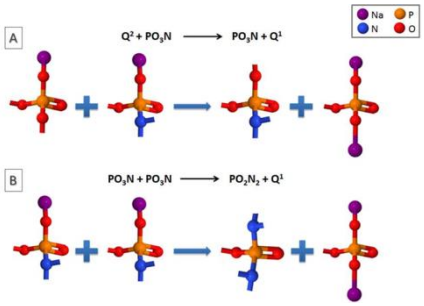

Figure 4-2. Suggested pressure induced conversions between structural units in the $NaPO_{3-3/2X}N_X$ oxynitride glasses, by exchange of a NBO-Na group with a nitrogen atom. (a) Conversion of a Q^2 unit and a PO_3N unit into a new PO_3N unit and a Q^1 unit. (b) Conversion of two PO_3N units into a PO_2N_2 and a Q_1 unit. Figure adopted from [72].

The experimental and calculated results show overall agreement. An unexpected result is however that the calculations show a net loss of Q^1 (-1.4 at%) in the $NaPO_{2.45}N_{0.37}$ glass. This indicates that Q^1 must be present in the uncompressed $NaPO_{2.45}N_{0.37}$ glass. Q^1 is present in the as-prepared $NaPO_3$ glass (4 at%), and small amounts of Q^1 units may remain in the glass upon nitridation.

Table 2. Experimental and calculated quantities of Q_1 and PO_3N units in the $NaPO_{3-3/2X}N_X$ glasses after compression. Calculated results are based on the suggested pressure reaction in Figure 4-2. Values of Q^2 and PO_2N_2 units are the same in experimental and calculated results. Table modified from [72].

Glass	Q^1 fraction (at.%)		PO_3N fraction (at.%)	
	exp.	calc.	exp.	calc.
$NaPO_3$ (1GPa)	4.0	4.0	0.0	0.0
$NaPO_{2.79}N_{0.14}$ (1GPa)		6.0	25.6	19.7
$NaPO_{2.64}N_{0.24}$ (1GPa)		3.8	39.1	35.3
$NaPO_{2.45}N_{0.37}$ (1GPa)		-1.4	46.0	47.4

4.2. MEDIUM RANGE ORDER

Changes in medium range order of hot compressed oxide glasses are not well understood. Previous studies on hot compressed SiO_2 glass have shown a change in ring statistics, with an increase in the fraction of smaller rings [20]. In borate glasses, a breakage of rings has also been found after compression [8][18][20][25].

The intermediate range order of borate glasses consists of ring structures with well-defined bond angles. We applied Raman spectroscopy and ^{11}B MAS NMR to study the structural changes in a sodium borate glass before and after hot compression [104]. A decrease in the fraction of ring-BO_3 was evident from both the Raman and ^{11}B MAS NMR spectra after compression, along with an increase in the fraction of non-ring BO_3. This indicates dissolution of rings during hot compression, as also previously suggested for v-B_2O_3 [116][122] [94] and an alkali borate glass [136].

Using ^{31}P MAS NMR, we studied the pressure induced changes in a $NaPO_3$ glass. The uncompressed glass consists of chains of Q^2 units terminated by Q^1 units. After compression, the only pressure induced changes observed was a shift to lower resonance frequency, i.e. no speciation changes were found.

Based on ^{31}P MAS NMR, we suggested a conversion of Q^2 units into Q^1 units after hot compression of a series of oxynitride glasses (see section 4.1.3). An increase of Q^1 units implicates an increase of terminal phosphate units on the chains in the glass network, i.e. a decrease in the average chain length and an increased number of chains.

4.3. COMPOSITION-PLASTIC COMPRESSIBILITY RELATIONS

The plastic compressibility of glass is fundamentally governed by its chemistry. Previous studies on hot compressed oxide glasses have mainly focused on isolated glass compositions [24][22][26][31][37], with only few studies on systematic variations of composition. One study on a calcium borate glass with varying Na_2O content showed a clear decrease in the plastic compressibility with increasing modifier content [24]. A recent study on the effect of substitution of modifier species (K_2O for Na_2O), with constant total modifier content, showed a decrease in the plastic compressibility with increasing $[K_2O]/([K_2O]+[Na_2O])$ [31]. Another study on the effect of modifier substitution (MgO for CaO), at constant total modifier content, found a mixed modifier effect (i.e. non-linear changes) in the plastic compressibility [30]. Such studies highlight the important influence of modifiers on the plastic compressibility of glass.

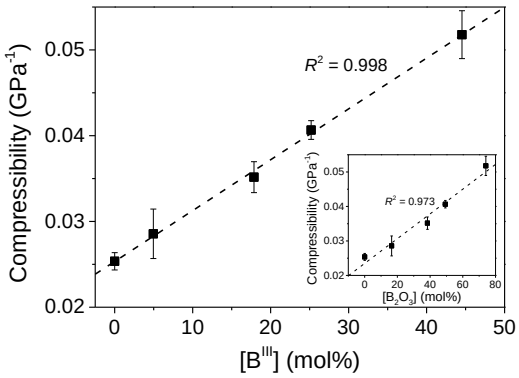

Figure 4-3. The concentration of BO_3 in a borosilicate glass series, plotted against the plastic compressibility of the glasses. The inset shows the relation between the total boron concentration ($[BO_3] + [BO_4]$) and the plastic compressibility, for the same borosilicate glass series. Figure adopted from [101].

To understand the relation between chemical composition and densification behavior, we performed two studies with systematic changes in chemical composition. These include a study on the effect of network former substitution (B for Si) in a borosilicate glass series [101], and a study on the effect of anion substitution (N for O) in a sodium methaphosphate glass [72]. Network former substitution is expected to show a large effect on the plastic compressibility of glasses. In Figure 4-3, the effect of varying boron concentration (B/Si) on the plastic compressibility of a borosilicate glass series is shown. From the inset of the figure, a linear correlation between boron concentration and plastic compressibility is seen. However, this relation is improved if only considering the BO_3 concentration in the

glass (main figure). The linear increase in plastic compressibility with increasing BO_3 concentration demonstrates the impact of network formers on the plastic compressibility. The linear relation across varying pressure-induced structural changes indicates that the plastic compressibility depends primarily on network former speciation (i.e. BO_3, BO_4 or SiO_2), as opposed to the medium range structures formed by these units.

We also studied the effect of anion substitution on the plastic compressibility of a series of $NaPO_{3-3/2X}N_X$ glasses. In Figure 4-4. the effect of increasing nitrogen concentration on the plastic compressibility is shown.

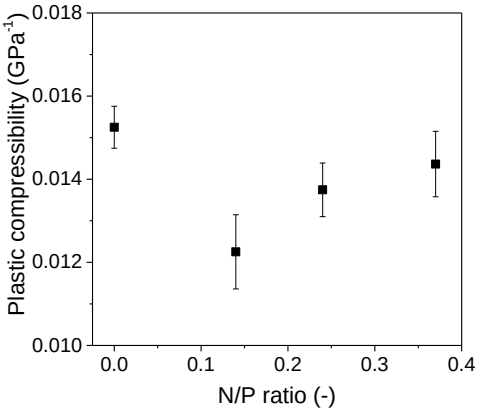

Figure 4-4. Plastic compressibility of a series of $NaPO_{3-3/2X}N_X$ oxynitride glasses plotted as a function of their nitrogen content (N/P ratio). Figure adopted from [72].

An initial decrease in the plastic compressibility is seen with increasing nitridation, which is reversed upon further nitridation. The plastic compressibility of the base $NaPO_3$ glass is very low, as well as for the nitrided glasses. The low plastic compressibility may be caused by the high modifier concentration in the base $NaPO_3$ glass, as it has previously been found that increasing modifier content significantly decreased the plastic compressibility of glass [24]. In turn, the low plastic compressibility of the base $NaPO_3$ glass may inhibit anion substitution from showing a clear effect on the densification behavior.

4.4. STRUCTURE AND DENSITY RELAXATION OF HOT COMPRESSED GLASSES

The pressure induced changes in density and properties can be relaxed by ambient pressure annealing. The relaxation time depends on the annealing temperature, and by selection of prober annealing temperatures, a step-wise monitoring of density and property relaxation can be performed. Only limited data on this type of experiments has been published and the relaxation behavior of compressed glasses is generally not well understood. For example, the timescale of density relaxation can currently not be predicted. However, an interesting observation is found when plotting data for density relaxation at $0.9T_g$ at ambient pressure, for glasses compressed at T_g at 1 GPa (see Figure 4-5). The relaxation times appear to follow a master curve, despite of the different chemistries of the glasses. However, further data is required to investigate whether this trend applies for further glass compositions.

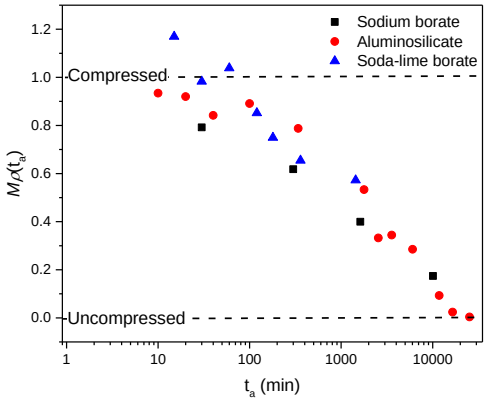

Figure 4-5. Relaxation function (see section 2.5) of three glasses during ambient pressure annealing at 0.9 T_g, after hot compression at 1 GPa at T_g. Data on soda-lime borate taken from ref [22], data on sodium borate taken from [104] and data on aluminosilcate glass taken from [105].

Understanding the structural changes during relaxation may also help to elucidate the structural origin of pressure induced density changes. To obtain a deeper understanding of structure-density relations, we compressed a sodium borate glass at 1 GPa at T_g, and monitored structural changes throughout relaxation by ^{11}B MAS NMR, ^{23}Na MAS NMR, Raman spectroscopy [104].

The BO_4 concentration of the samples throughout density relaxation is shown in Figure 4-6. It can be seen that BO_4 concentration followed density throughout relaxation. The figure also shows an uncompressed sample, subjected to prolonged annealing at 0.9 T_g, at ambient pressure. This sample shows that the BO_4 concentration changes more as a function of density, when densification is obtained through changes in thermal history, as compared to changes in pressure history.

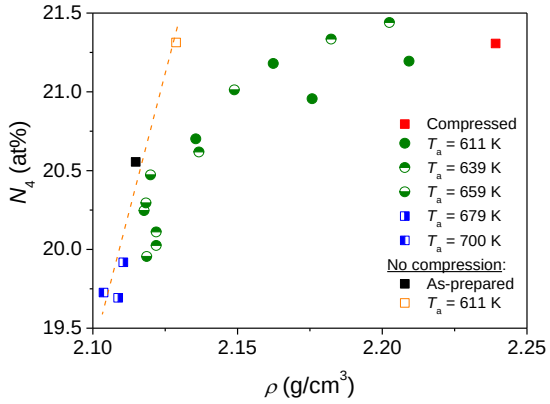

Figure 4-6. BO_4 concentration in the compressed samples throughout relaxation, as quantified by ^{11}B MAS NMR. Included for comparison are also an uncompressed glass, annealed at 0.9 T_g (K) for 168 Hrs and the as-prepared glass. The inserted line represents changing fictive temperature for glasses without pressure effects. Figure adopted from [104].

Figure 4-7 shows the ring to non-ring BO_3 ratio of the same samples. From the figure it can be seen that the ring/non-ring BO_3 ratio decreased after hot compression, but that the ratio also decreased in a similar manner with increasing T_f. Hereby, the same ring/non-ring BO_3 ratio can be obtained across various densities. As similarly seen for the BO_4 concentration, the rate of change in the ring/non-ring fraction as a function of density is also higher when changes are imposed by variations in the thermal history, rather than pressure-temperature history.

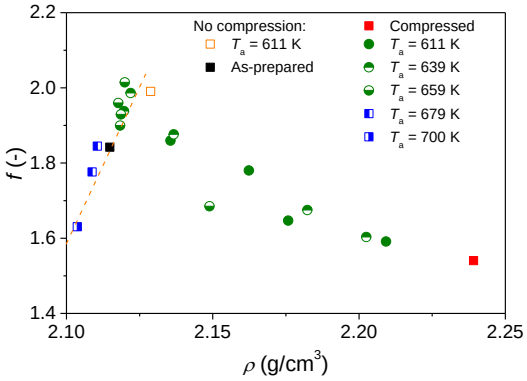

Figure 4-7. The ring/non-ring BO_3 ratio of the compressed samples throughout ambient pressure relaxation, as quantified by ^{11}B MAS NMR. Included for comparison are also an uncompressed sample, annealed at 0.9 T_g (K) for 168 Hrs and the as-prepared sample. The inserted line represents changing fictive temperature for glasses without pressure effects. Figure adopted from [104].

The changes in the ^{23}Na MAS shift were also monitored throughout relaxation. The results are shown in Figure 4-8.

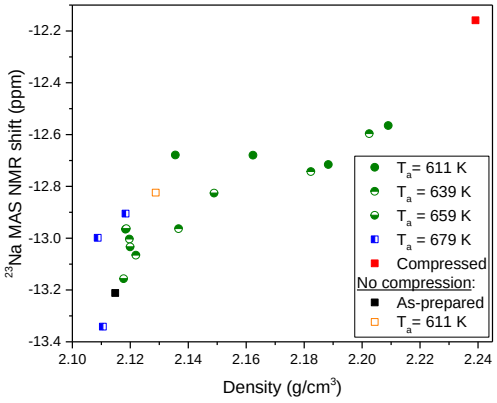

Figure 4-8. ^{23}Na MAS shift of the compressed samples throughout ambient pressure relaxation, as quantified by ^{23}Na MAS NMR. Included for comparison are also an uncompressed glass, annealed at 0.9 T_q (K) for 168 Hrs and the as-prepared glass. Figure adopted from [104].

From the figure it can be seen that the ^{23}Na MAS shift moved to higher frequency after compression. During relaxation, it gradually relaxed towards the uncompressed value. It can also be seen that the value of the uncompressed sample, sub-T_g annealed at ambient pressure for 168 Hrs, aligned with the trends of the compressed and relaxed samples. This is in contrast to the BO_4 concentration and the ring/non-ring BO_3 ratio, for which a different relation with density was seen for compressed-relaxed samples and the as-prepared sample sub-T_g annealed at ambient pressure for 168 Hrs.

4.5. SUMMARY

We monitored pressure-induced structural changes after compression at T_g in an aluminosilicate [104][105], a sodium borate [104], a borosilicate [101] and a series of oxynitide methaphosphate glasses [72]. We found densification of glasses to be accompanied by a compaction of modifier environments, coordination changes of network formers and changes in intermediate range structures (e.g. rings). We further suggested a pressure reaction for the oxynitride glasses, primarily causing an increase in Q^1 units after hot compression. We also monitored changes in BO_4 concentration, ring/non-ring BO_3 ratio and ^{23}Na environment during relaxation of a hot compressed sodium borate glass [104]. For the BO_4 concentration and the ring/non-ring BO_3 ratio, it was found that similar changes could be obtained across varying density, depending on the densification method, indicating that these structural parameters do not govern bulk density of the glass. Changes in the ^{23}Na environment however followed density throughout ambient pressure relaxation.

An interesting observation was also made when plotting relaxation times of density during ambient pressure 0.9 T_g annealing, for three different glasses compressed at T_g. Relaxation times were found to align to a master curve, despite of the glasses having different compositions and compressibilities. The cause of this alignment in relaxation times is not understood.

CHAPTER 5. HARDNESS AND ELASTIC PROPERTIES OF HOT COMPRESSED GLASSES

Improving the mechanical properties of glass is a key issue for enabling future technological applications [25]. The structural basis of properties such as hardness, crack resistance and brittleness are however not well understood, and predictive models for hardness have only been applied within limited compositional regimes [76][77][12]. Compression can modify the mechanical properties of glass, but the structural basis for this modification is not well understood. It is therefore relevant to obtain a deeper understanding of the pressure-induced changes in mechanical properties of glass.

5.1. PRESSURE INDUCED INCREASE IN H_V AND ELASTIC MODULI

Pressure compaction increases the hardness of glass [22][24][93][30]. The pressure induced increase in H_v has previously been found to scale with the pressure induced density increase, for various glass compositions [22][24][93].

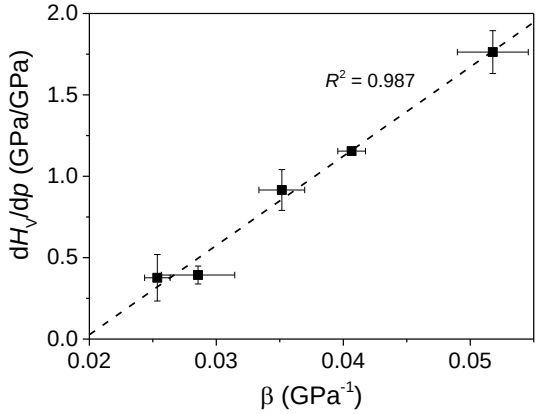

Figure 5-1. Relative increase in hardness (dH_v/dP) plotted as a function of plastic compressibility (β), determined after hot compression at T_g and 1 GPa, for a series of borosilicate glasses with constant modifier content. Figure adopted from [101].

By studying the pressure induced increase in hardness and density across a series of borosilicate glasses, we found a linear relation between the relative changes in density and hardness (see Figure 5-1). That a constant relation between the pressure-induced increase in hardness and density applies, across varying compositions, indicates that these changes are rooted in fundamental physical relations between density and hardness. This aligns with our findings on the pressure induced changes in elastic moduli of hot compressed glasses [100] (cf. Figure 5-2), where we demonstrated a common relation between the pressure induced changes in elastic moduli and density across a variety of oxide glass compositions. Hardness and elastic moduli are known to correlate [74][137][76], so an increased hardness is also expected from an increased elastic moduli, i.e. the trends of Figure 5-1 and Figure 5-2 are mutually supportive**.**

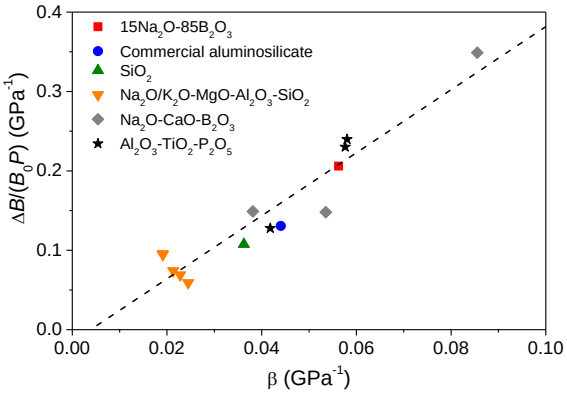

Figure 5-2. The normalized changes in bulk modulus ($\Delta B/(B_0P)$) as a function of plastic compressibility (β) for various glass compositions compressed at their respective ambient pressure T_g values. The dashed line represents a least squares linear fit (R^2=0.90) to the data (intercept equal to -0.015±0.018 and slope equal to 3.97±0.39). Figure adopted from [100].

This is further supported by a recent compilation on the relative changes in hardness and density after hot compression (cf. Figure 5-3). Across the borosilicate glass series, and the glasses included in Figure 5-2 and Figure 5-3, a variety of structural changes occur upon compression. Despite the details of the pressure induced structural changes, the common relations between hardness, elastic moduli and density indicate that a fundamental physical relation between these properties exists.

It is interesting whether the correlation between relative changes in density and hardness of hot compressed oxide glasses also applies to oxynitride glasses. We studied the pressure induced changes in density and hardness of a series oxynitride methaphosphate glasses [72]. The effect of compression on density and hardness is shown in Figure 5-4.

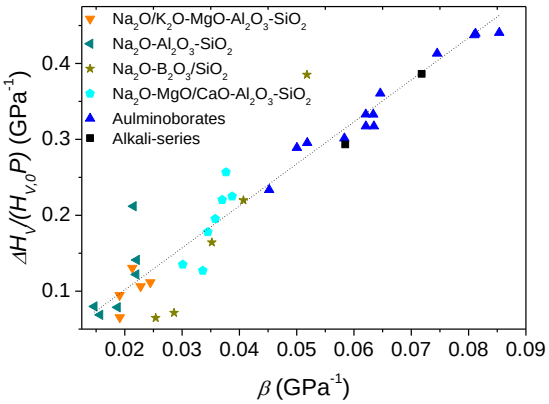

Figure 5-3. Relative changes in hardness (dHv/Hv,0P) plotted against the plastic compressibility (β) for a variety of glass compositions after hot compression. Figure adopted from [138]. Inserted line represents a least squares linear fit to the data.

The changes in density and hardness correlate, indicating that similar relations between densification and hardness also apply for oxynitride glasses. However, it should be noted that the pressure induced changes in hardness and density for the oxynitride glasses are very small.

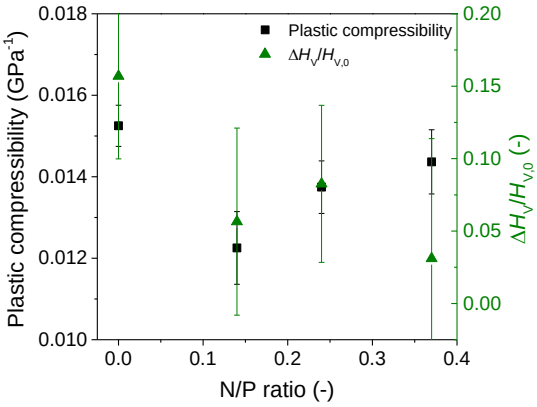

Figure 5-4. Pressure induced changes in density and hardness for a series of $NaPO_3$-$_{3/2X}N_X$ oxynitride glasses, plotted against their nitrogen content (N/P ratio). Figure adopted from [72].

Despite of the relation between hardness and density appearing to indicate a physical relation between these parameters, it is unlikely that this is the explanation. During ambient pressure sub-T_g annealing of hot compressed glasses, the pressure-induced density and hardness changes have been found to de-couple in relaxation times [22]. This indicates that the hardness is not governed by the density, but rather by specific pressure-induced structural changes. That specific structural changes are important for the changes in mechanical properties is further illustrated by comparing the changes in longitudinal wave velocity with changes in density, when densification is obtained by hot compression or ambient pressure sub-T_g annealing (cf. Figure 5-5).

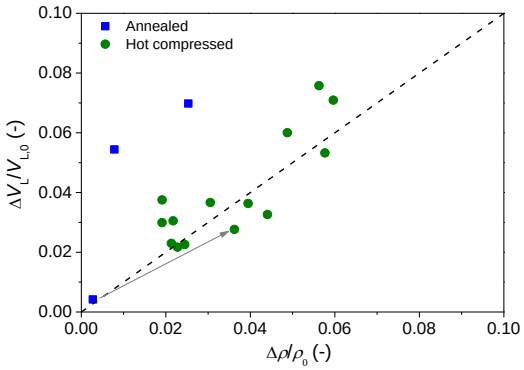

Figure 5-5. Relative changes in longitudinal wave velocity and density, for samples densified through ambient pressure sub-T_q annealing or hot compression. The inserted arrow connects two samples of identical composition (SiO_2). Figure adopted from [100].

The longitudinal wave velocity is proportional to the elastic moduli, and used here since more data was available from the literature on this parameter. If the changes in longitudinal wave velocity were only governed by density, the trends for both densification methods would overlap. These trends do however not overlap. Instead, the relative changes in longitudinal wave velocity are higher, as a function of relative density increase, when densification is obtained by ambient pressure sub-T_g annealing than by hot compression. This aligns with the hardness increasing more as a function of density, when densification is obtained by ambient pressure sub-T_g annealing, instead of hot compression [84][85]. This indicates that specific structural changes occurring during ambient pressure sub-T_g annealing and hot compression govern the changes in elastic moduli. A difference in bulk modulus has also been found for SiO_2 glasses densified equally through hot- or cold compression [20].

5.2. CHEMICAL STRENGHTENING AND HOT COMPRESSION

Chemical strengthening, also referred to as ion exchange, is a method widely applied in industry for the strengthening of glasses for e.g. cockpit windows and display covers in personal electronic devices. The treatment is performed by producing a glass with a small ion (e.g Na^+) included in the melting batch. After melt-quenching, the glass is submerged into a salt bath (e.g. KNO_3) at elevated temperature, where the smaller ion (e.g. Na^+) is substituted with a larger ion (e.g. K^+) through inter-diffusion. Inclusion of the larger ion, into sites previously occupied by the smaller ion, causes a local expansion of the ion site [139]. This structural modification causes a compressive stress in the glass surface, which is balanced by a tensile stress in the interior of the glass. The compressive surface stress inhibits the formation and propagation of cracks, increasing the damage resistance of the glass. The treatment also increases the hardness of the glass (as measured on the glass surface).

We investigated the impact hot compression combined with ion exchange on the hardness of a commercial aluminosilicate glass. The glass was either submitted to ion-exchange and then hot compression (post-compression), or first submitted to hot compression and then ion exchanged (pre-compression). We found that post-compression did not modify the hardness when compression was performed at low temperature (i.e. below 450 ^oC). However, raising the compression temperature caused diffusion of K^+ ions in the glass surface during compression, causing a decrease in K^+ surface concentration which decreased the hardness of the glass (see Figure 5-6).

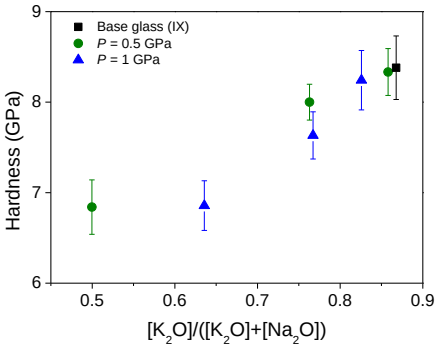

Figure 5-6. Hardness and K^+ concentration in the surface layer of samples subjected to ion exchange (10 Hrs in KNO_3 salt bath at 410 ^oC) followed by compression at various temperatures for 0.5 Hrs. A relation between K^+ surface concentration and hardness is seen. Figure adopted from [102].

In contrast, pre-compression was found to increase the hardness of the glasses. The changes in hardness for samples compressed and ion exchanged were found to scale with the pressure induced changes in Na^+ environment, as quantified by ^{23}Na MAS NMR. Figure 5-7 shows the changes in hardness as a function of ^{23}Na δ_{CS} . The plot includes pre-compressed and post-compressed samples, as well as a pristine sample sub-T_g annealed for 168 Hrs followed by ion exchange.

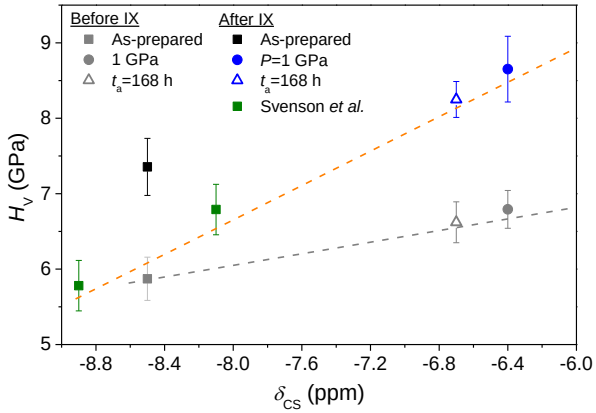

Figure 5-7. Hardness as a function of ^{23}Na chemical shift (δ_{CS}) for samples before (grey symbols) and after (colored symbols) ion exchange (IX). ^{23}Na δ_{CS} was measured on ion exchanged samples and assumed also to apply similarly for samples before ion exchange. This assumption is supported by MD simulations [139], which found ion exchange not to cause significant changes in the Na^+ environment. The dashed lines are guides for the eye. Figure adopted from [114].

Across all the samples (with one exception) the changes in hardness are found to scale with the changes in ^{23}Na chemical shift. It is interesting that a common relation applies for the glasses, across the different densification methods. Sub-T_g annealed samples normally exhibit a different hardness vs. density relation than hot compressed samples [102][103]. This indicates that the chemical shift does not only depend on the density, but rather on specific structural changes closely related to hardness.

5.3. COMBINED EFFECT OF HOT COMPRESSION AND SUB-T_G ANNEALING ON GLASS HARDNESS

Hot compression and ambient pressure sub-T_g annealing can increase the hardness and density of glasses [84][85]. However, the hardness increase obtained by ambient pressure sub-T_g annealing is higher, as function of density, than that obtained by hot compression [114]. This indicates that different structural mechanisms operate during the two densification methods. Comparative studies on the effect of ambient pressure sub-T_g annealing and hot compression are few [114][140]. The structural changes resulting from ambient pressure sub-T_g annealing and hot compression have recently been studied using molecular dynamics simulations [114]. Here it was suggested that ambient pressure sub-T_g annealing mainly causes changes in short range order, whereas hot compression mainly causes changes medium range order.

We have made a comparative structural analysis of a commercial sodium aluminosilicate glass after hot compression and ambient pressure sub-T_g annealing. The results can be seen in Figure 3-2 in section 3.1. From the figure it can be seen that ambient pressure sub-T_g annealing and hot compression caused opposing changes in the ^{23}Na MAS NMR shift and ^{27}Al isotropic chemical shift, confirming that fundamentally different structural changes occur under these two densification methods.

Due to the different structural mechanisms causing the same qualitative changes in hardness and density, it was found interesting whether sub-T_g annealing and hot compression could be combined. Combining these two methods in sequence is however difficult, since the effects of one treatment cancels the effects of the other treatment (e.g. ambient pressure sub-T_g annealing causes relaxation of pressure induced property changes). Instead we combined hot compression and sub-T_g annealing by performing sub-T_g annealing *in situ* under pressure (1 GPa), after compression at T_g at 1 GPa. The procedure is described in Figure 2-8. First, the samples were conventionally hot compressed (T_g, 1 GPa, 30 min). Then, pressure was kept constant while the temperature was lowered to 0.9 T_g. Hereby, sub-T_g annealing was performed *in situ* (1 GPa) for durations of 2 Hrs or 24 Hrs, followed by cooling and decompression. The density of the samples are shown in Figure 5-8., along with the densities of uncompressed samples annealed at 0.9 T_g for the same durations. The combination of compression at T_g and *in situ* sub-T_g annealing caused an increased density. Furthermore, the density increase as a function of annealing time was similar, regardless of the pressure applied. Sub-T_g annealing at different pressures also affected the hardness of the glasses, as shown in Figure 5-9. The figure shows that ambient pressure sub-T_g annealing resulted in a different hardness-density relation than hot compression, with an equivalent effect on hardness regardless of the pressure apllied during sub-T_g annealing. Furthermore, increasing the annealing time at T_g and 1 GPa did not alter the density or hardness of the samples.

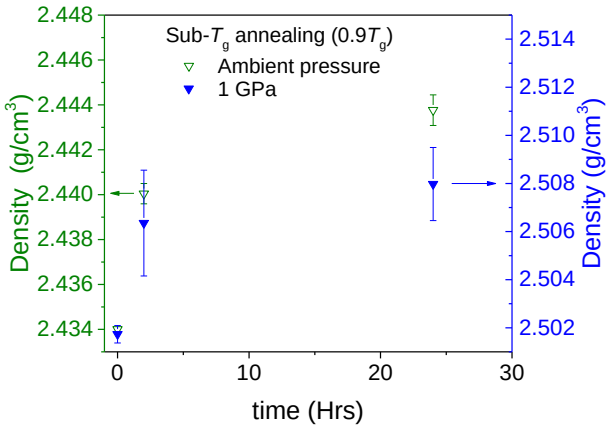

Figure 5-8. Density of pristine samples after annealing at 0.9 T_g (ambient pressure) and hot compressed samples after annealing at 0.9 T_g (1 GPa). Figure adopted from [105].

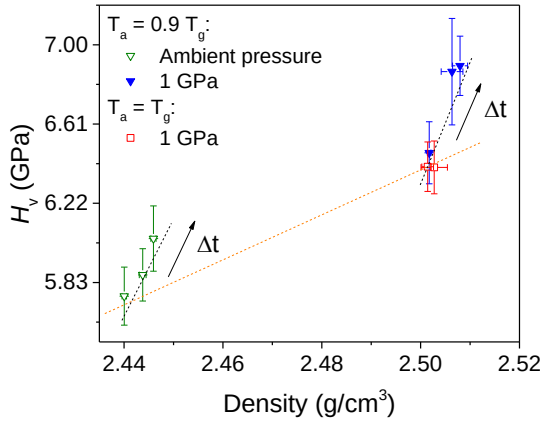

Figure 5-9. Hardness and density of uncompessed samples annealed at 0.9 T_g, samples annealed at T_g and 1 GPa for various durations, and samples annealed at T_g and 1 GPa followed by annealing at 0.9 T_g at 1 GPa Arrows denote increasing annealing time at 0.9 T_g. All three sets of samples were annealed for 0, 2, or 24 Hrs. The inserted orange line shows hardness-density relation of samples without sub-T_g annealing (i.e. effect of hot compression). Inserted black lines show hardness-density relation as a function of sub-T_g annealing. Figure adopted from [105].

5.4. HARDNESS RELAXATION IN HOT COMPRESSED GLASSES

A decoupling between the timescales of density and hardness relaxation has previously been found for hot compressed glasses [22]. However, only limited data is available for this type of experiment, so for further investigation of this phenomenon, we investigated the relaxation times of hardness and density in a hot compressed silicate glass [101]. In Figure 4-8 the relaxation function and the strecthed exponential fit (described in section 2.5) are plotted for the density and hardness during ambient pressure relaxation.

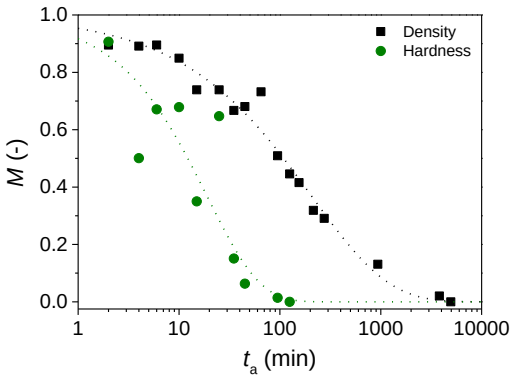

Figure 5-10. Relaxation function (M) and Kolsrauch fit ($M(t_a)$) for density and hardness of a hot compressed silicate glass during ambient pressure annealing at 0.92 T_g. Figure adopted from [101].

The figure shows that hardness and density relax at different timescales, as previously observed for another compostion [22]. To compare the timescales of hardness relaxation for different glass compostions, hot compresed glasses relaxed at the same relative T_g temperature (0.9 T_g) are plotted in Figure 5-11. The glasses were compressed at T_g and 1 GPa (aluminosilicate glass) or 0.57 GPa (borate glass) prior to ambient pressure relaxation. The figure shows that time scales for hardness relaxation of the two glasses do not clearly overlap, as was found for density relaxation (see Figure 4-5). However, hardness measurements usually have higher uncertainty than density measurements, and there is significant scatter in the hardness data, so no conclusion is drawn from this data.

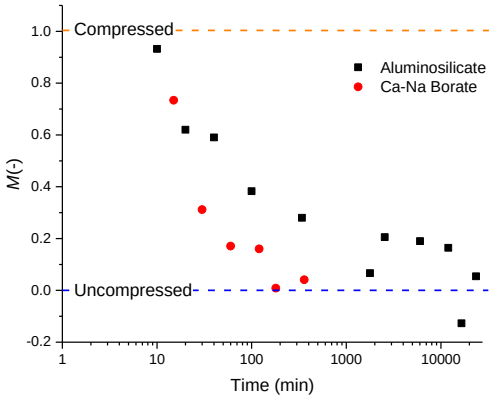

Figure 5-11. Relaxation function (M) (see section 2.4.3 for description) for the hardness of an aluminosilicate glass [105] and a borate glass [22] during ambient pressure sub-Tg annealing (0.9 T_g).

As described in section 5.3, we investigated glasses subjected to hot compression followed by *in situ* (1 GPa) sub-T_g (0.9 T_g) annealing. This type of treatment was found to successfully combine the effects of hot compression with the effects usually seen from ambient pressure sub-T_g annealing. Because the two treatment methods modify the density and hardness through different structural mechanisms, it was found interesting to investigate the relaxation behavior of glasses with the effects of both treatments combined. The results are shown in Figure 5-12. The glass compressed by conventionally hot compression (T_g, 1 GPa) showed a decoupling between density and hardness during relaxation. This aligns with previous results [22]. However, the samples also subjected to *in situ* (1 GPa) sub-T_g annealing (0.9 T_g) did not show this decoupling. This is a surprising finding and might indicate a coupling between the structural parameters governing hardness and those governing density, after this type of treatment. A recent molecular simulations study on the effects of hot compression and ambient pressure sub-T_g annealing found hot compression to affect primarily medium range order, whereas sub-T_g annealing modified primarily short range order [114]. A possible explanation is that hot compression causes compaction resulting in some elements being positioned in setting with weak bonding. Sub-Tg annealing may allow for changes in the bond environment within these settings, causing increased network connectivity and a coupling between relaxation processes of different parts of the glass network.

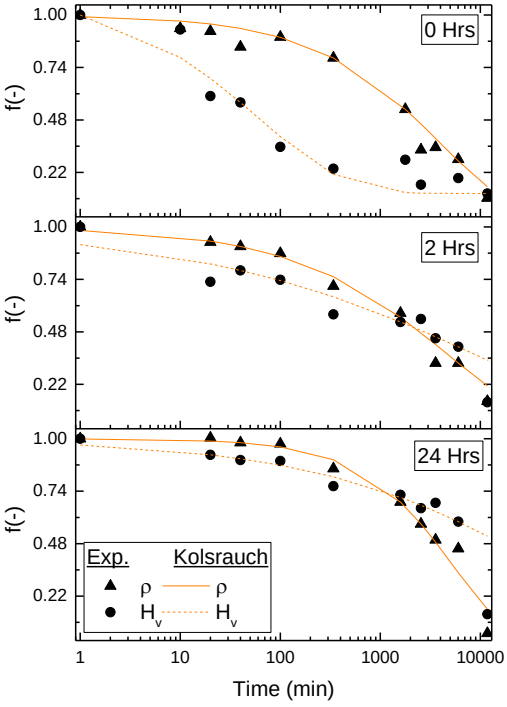

Figure 5-12. Relaxation function (M) and Kolsrauch fit ($M(t_a)$) for density and hardness throughout ambient pressure relaxation at 0.9 T_g. Prior to relaxation, all samples were compressed at T_g (1 GPa). This was followed by annealing at 0.9 T_g (1 GPa), for durations of a) 0 Hrs, b) 2 Hrs, c) 24 Hrs (compression protocol described in section 2.4.3.) Figure adopted from [105].

5.5. SUMMARY

Compression at T_g increases the density, hardness and elastic moduli of glasses with a constant relation between the relative changes in density, hardness and elastic moduli. This indicates a fundamental physical relation between these changes. However, relaxation experiments show that the timescales of hardness and density relaxation decouple during ambient pressure annealing, indicating that these parameters are not mutually dependent. Furthermore, we also find that change in longitudinal wave velocity (proportional to elastic moduli) dependent on the densification method applied, and not just the density. This again indicates that changes in elastic moduli depend on specific structural changes in the glasses, rather than just density.

Ion exchange of hot compressed glasses resulted in a higher hardness than ion exchange on uncompressed glasses. The hardness increase resulting from hot compression, with and without ion exchange, could be related to pressure-induced changes in the ^{23}Na environment. Based on these results, it is suggested that a more compacted ^{23}Na site causes a larger increase in hardness after ion exchange. This can be understood by the K^+ ion substituted into the Na^+ site exerting a larger pressure on the glass network when the Na^+ site is compacted. This may in turn increase the compressive stress in the glass surface, resulting in an increased hardness.

By combining hot compression with *in situ* (1 GPa) sub-T_g (0.9 T_g) annealing, an increased density and hardness could be obtained. Hot compression and sub-T_g annealing have previously been suggested to cause different structural changes in the glass network [114]. This is supported by our findings. Furthermore, by combining hot compression with *in situ* (1 GPa) sub-T_g annealing (0.9 T_g), the relaxation behavior of the glasses was modified. The decoupling between timescales of density and hardness relaxation previously found for hot compressed glasses was diminished when additional *in situ* sub-T_g annealing was also applied.

CHAPTER 6. GLASS TRANSITION BEHAVIOR OF HOT COMPRESSED GLASSES

The glass transition is fundamental for defining a solid as a glass. It has previously been found that hot compression affects the glass transition behavior of glasses [25][36]. Investigating the changes in glass transition behavior of compressed glasses may aid to further understand the impact of compression on glass structure and properties. For example, glasses equivalent in boron coordination and molar volume, tailored by compression or ambient pressure cooling rate, have been suggested to differ in mid- or long range structural arrangements, based on differences in T_f and enthalpy overshoot [112]. Investigating the changes in glass transition behavior during relaxation of compressed glasses may also be important in order to further understand the relaxation behavior of compressed glasses. Differential Scanning Calorimetry (DSC) is a useful method for characterization of the glass transition behavior. From DSC scans parameters such as T_f, enthalpy overshoot and ΔT_g can be quantified (see section 2.1 for description). DSC measurements on hot compressed glasses have previously found hot compression to cause an increase in the enthalpy overshoot [101][31][22][46] and changes in T_f. Typical changes in the glass transition region imposed by compression are shown in Figure 6-1.

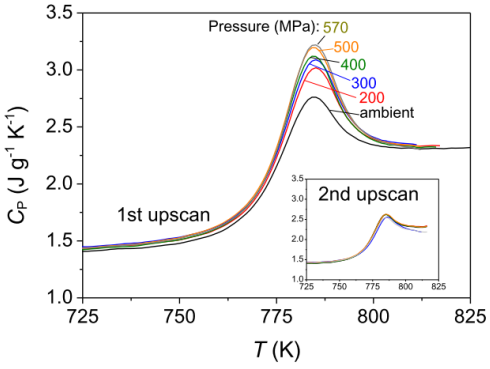

Figure 6-1. First DSC scans of a borate glass hot compressed at T_g at various pressures up to 0.57 GPa. The inset shows the 2nd DSC scan of each sample, i.e. scans after full relaxation of pressure induced structural changes. Figure adopted from [22].

A previous study on hot compressed aluminosilicate glasses found interesting relations between the pressure-induced changes in the glass transition behavior, and the plastic compressibility. Figure 6-2 shows pressure induced changes in enthalpy overshoot and T_f for a series of aluminosilicate glasses with constant modifier content, but varying $[K_2O]/([K_2O+Na_2O])$.

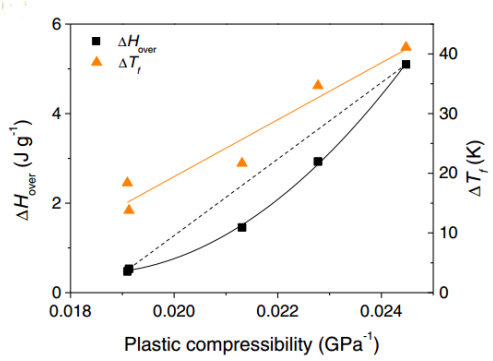

Figure 6-2. Relative changes in enthalpy overshoot and ΔT_f after compression at T_g at 1 GPa, for a series of aluminosilicate glasses with varying $[K_2O]/([K_2O+Na_2O])$. Figure adopted from [31].

From the figure a trend between the pressure-induced changes in density, enthalpy overshoot and fictive temperature is seen. These types of relations between pressure-induced changes in the glass transition behavior and density may provide increased understanding on the pressure-induced structural changes after hot compression.

6.1. IMPACT OF HOT COMPRESSION AND SUB-T_G ANNEALING ON GLASS TRANSITION BEHAVIOR

We used DSC to study the impact of sub-T_g annealing on the glass transition behavior of an uncompressed and a hot compressed glass. Sub-T_g annealing and hot compression have previously been suggested to densify glasses through different structural mechanisms [114]. Both methods also cause changes in the glass transition behavior. We subjected two set of samples to either ambient pressure annealing at 0.9 T_g, or compression at T_g and 1 GPa, followed by annealing at 0.9 T_g and 1 GPa (as described in section 2.4.3). DSC scans of the samples can be seen in Figure 6-3. The figure shows that hot compression (T_g, 1 GPa) caused an increase in the enthalpy overshoot. Sub-T_g annealing similarly caused an increase in the enthalpy overshoot for both the uncompressed and the hot compressed sample. The enthalpy overshoot did not increase by longer annealing time at T_g and 1 GPa.

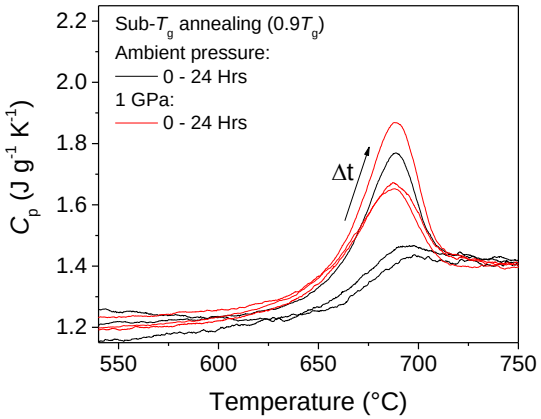

Figure 6-3. DSC scans of an aluminosilicate glass annealed at ambient pressure at 0.9 T_g, or compressed at T_g at 1 GPa, followed by annealing at 0.9 T_g at 1 GPa. For both set of samples, sub-T_g annealing times were; 0 Hrs, 2 Hrs or 24 Hrs. The inserted arrow denotes increasing annealing time. Figure adopted from [105].

The increase in the enthalpy overshoot resulting from sub-T_g annealing shows that the effect of sub-T_g annealing applies similarly to glasses under different pressures, and furthermore, it shows that sub-T_g annealing and hot compression causes different changes in the glass transition behavior (i.e. structure of the glass). That sub-T_g annealing causes a similar increase in the enthalpy overshoot at different pressures aligns with previous results showing that the impact of cooling rate on BO_4 concentration in a borosilicate glass was pressure-independent [112].

6.2. IMPACT OF RELAXATION ON GLASS TRANSITION BEHAVIOUR

Little is known about the changes in the glass transition behavoir during relaxation of hot compressed glasses. A thermodynamic understanding of the relaxation behavior may however improve our understanding of the relaxation process. For example, the fundamental question of whether full relaxation of pressure induced structure and property changes can be achieved by ambient pressure sub-T_g annealing remains unanswered. It has previously been found that full relaxation of pressure induced structural changes (i.e. BO_4 concentration), was not obtained by ambient pressure annealing at 0.9 T_g [22].

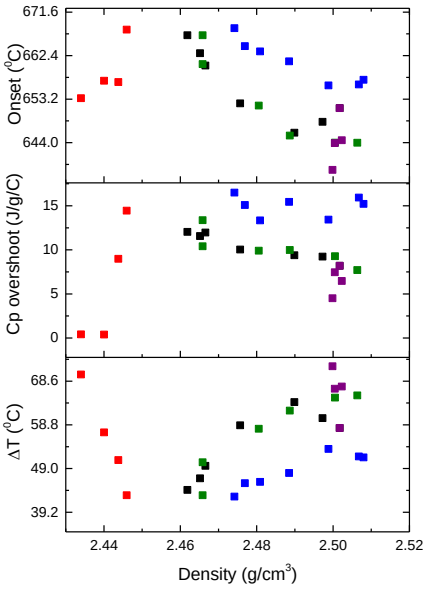

Figure 6-4. Glass transition onset temperature, enthalpy overshoot and ΔT_g during ambient pressure 0.9 T_g annealing of; an uncompressed sample (red squares), a sample compressed at T_g at 1 GPa (black squares), and samples hot compressed followed by annealing at 0.9 T_g and 1 GPa for 2 Hrs (green squares) or 24 Hrs (blue squares). Purple squares show samples hot compressed (T_g, 1 GPa) for durations up to 24 Hrs. Figure adopted from [105].

Using DSC, we investigated the glass transition behavior during relaxation of a hot compressed aluminosilicate glass, and glasses subjected to hot compression followed by i*n situ* sub-T_g annealing (see section 2.4.3). We studied the changes in apparent onset temperature, enthalpy overshoot and ΔT_g during prolonged ambient pressure annealing at 0.9 T_g. The changes in thermodynamic properties as a function of density are shown in Figure 6-4. Relaxation caused each glass to approach the same values for these parameters regardless of prior treatment. This indicates that full relaxation of all the samples was obtained. In section 6.1 it was described how *in situ* (1 GPa) sub-T_g annealing (0.9 T_g) caused changes in the glass transition behavior, as a function of annealing time. From Figure 6-4 it can be seen that the changes resulting from different *in situ* annealing times remained pronounced throughout relaxation. Furthermore, it can be seen that equivalent changes in the thermodynamic properties was achieved across various densities, i.e. these properties are relatively density independent. This points towards specific structural changes governing the changes in the glass transition behavior

6.3. SUMMARY

Hot compression causes marked changes in the glass transition behavior, including an increase in the enthalpy overshoot, a decrease in the glass transition onset temperature and an increase in ΔT_g. By perfoming *in situ* sub-T_g annealing (0.9 T_g) under pressure (1 GPa), similar effects can be imposed on the glass transition behavior as during ambient pressure sub-T_g annealing (0.9 T_g). This indicates that hot compression and sub-T_g annealing affects the structure differently, and that sub-T_g annealing has a remarkably similar effect on glass at ambient pressure and elevated pressure (1 GPa). Relaxation experiments of hot compressed glasses with- and without *in situ* sub-T_g anneling (0.9 T_g) showed that the effects of *in situ* sub-T_g annealing remains pronounced in the glasses throughout relaxation. Furthermore, changes in the glass transition behavior indicate that full relaxation of the samples is achieved after prolonged ambient pressure sub-T_g annealing, regardless of the prior treatment of the glass. The glasses relax towards the state of an uncompressed glass subjected to prolonged sub-T_g annealing at ambient pressure (i.e. low fictive temperature).

CHAPTER 7. DISCUSSION ON DENSIFICATION MECHANISMS

Pressure-induced structural changes have been reported in a variety of glasses densified through hot- or cold compression, but relations between structure and density remain relatively unclear. Furthermore, the influence of physical properties (e.g. T_g and hardness) on the plastic compressibility of glasses is not well understood either. In the following, relations between physical characteristic of glasses and pressure-induced changes in structure and density will be discussed.

7.1. STRUCTURAL BASIS OF DENSIFICATION BY HOT COMPRESSION

For all cases of hot compressed glasses we have investigated with ^{23}Na MAS NMR, a shift of the ^{23}Na resonance frequency to higher frequency has been found. A similar shift of ^{23}Na resonance frequency has previously been found in a variety of hot compressed oxide glasses [22][95][125][113]. This shift to higher resonance frequency has been interpreted as a shortening of the Na-O bond length [95]. This indicates a compaction of the modifier environment upon compression, possibly causing densification. However, recent results have shown that increasing modifier content dramatically decreases the plastic compressibility of a borate glass [24], i.e. indicating that compaction of modifier sites is not the dominant densification mechanism. Network modifiers occupy the interstices of the glass network, which in turn indicates that compaction of interstitial sites is an important part of the densification process. Known pressure induced structural changes include changes in intermediate range order (e.g. a conversion between ring and non-ring structures) and coordination changes of network formers (e.g. conversion from B^{III} to B^{IV}). It is therefore relevant to consider whether these structural changes could govern pressure-induced densification.

Based on differences in the partial molar volumes, it has previously been found for a pressure quenched aluminoborosilicate [95] and aluminosilicate glasses [125][113] that coordination changes of boron and aluminum could not account for overall densification. Furthermore, a recent study on a hot compressed soda-lime borate glass also found that coordination changes remained constant throughout density relaxation [22]. Coordination changes are therefore only expected to account for a fraction of the density changes after hot compression.

Using ^{11}B MAS NMR and Raman spectroscopy, we found that compression caused a conversion between ring BO_3 and non-ring BO_3 in a sodium borate glass. However, the same conversion could be achieved by increasing the fictive

temperature of the glass at ambient pressure (i.e. by decreasing density)(cf. Figure 4-7). This indicates that the conversion between ring and non-ring BO_3 was not the dominant pressure-induced densification mechanism, i.e. intermediate range order did not correlate with density.

Based on the above, it is considered unlikely that pressure-induced compaction of modifier sites, changes in coordination numbers, or conversions between intermediate range structures are the dominant densification mechanisms in hot compressed glasses, although they likely all contribute. We therefore infer that packing of network forming units, rather than conversions between structural units, is the primary cause of pressure-induced densification. This is expected to occur primarily through changes in the oxygen linkages connecting network polyhedra (e.g. bond angles). A decrease in network bond angles (i.e. Si-O-Si and Si-O-Al) has also previously been suggested to occur in hot compressed oxide glasses, based on relatively small shifts in ^{27}Al and ^{29}Si MAS resonance frequencies [125]. Similarly, a decrease in bond angles has also been suggested in pressure densified SiO_2 [141], alkali silicates and aluminosilicates [37].

The suggestion that packing of structural units should govern the density increase in hot compressed glasses also agrees with our comparative study of hot- and cold compressed sodium borate glass [110]. Here it was inferred that the mechanism governing density of the glass was not observed by Raman spectroscopy (i.e. changes in the packing of structural units could be such a mechanism). It also agrees with our study on a $NaPO_4$ glass, where we found that densification was achieved without any speciation changes, indicating that packing of structural units, rather than conversion between structural units, appear to be the dominant densification mechanism. Pressure-induced packing of structural units has also previously been suggested as the main densification mechanism for v-B_2O_3 [17].

If oxygen linkages between network forming polyhedra are the main controller of pressure-induced densification, it is relevant to consider structural techniques capable of monitoring changes in the oxygen environment. ^{17}O NMR has previously been applied to study pressure-induced structural changes in hot compressed sodium silicate [129] and aluminosilicate glasses [37][130][124]. For all the glasses, compression caused a significant shift to lower frequency in the isotropic dimension [129] [130] [124]. This shift has been suggested to be caused by an increased bond length (e.g. Al-O and Si-O) and a decrease in angles between network polyhedra [124]. Similarly, a pressure-induced decrease in angles between network polyhedra has also previously been suggested for aluminosilicate glasses, based on ^{17}O MAS NMR [37].

7.2. PHYSICOCHEMICAL BASIS OF Ddensification BY HOT COMPRESSION

Besides the structural aspect of densification, it is also interesting to consider the physics governing the process. When looking at parameters typically used to characterize glasses, such as density and T_g, no apparent relation with plastic compressibility is found (see Figure 7-1).

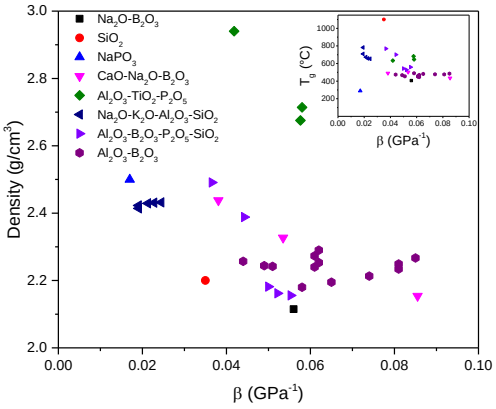

Figure 7-1. Density plotted against the plastic compressibility (β) for a variety of glass compositions. Inset: Glass transition temperature (T_g) plotted against the plastic compressibility (β). Data taken from: Na_2O-B_2O_3 [104], SiO_2 [142], $NaPO_3$ [72], CaO-Na_2O-B_2O_3 [24], Al_2O_3-TiO_2-P_2O_5 [143], Na_2O-K_2O-Al_2O_3-SiO_2 [31], Al_2O_3-B_2O_3-P_2O_5-SiO_2 [144], Al_2O_3-B_2O_3 [138].

Density is a product of both mass and volume of the glass network. For a purely structural approach, it might be more relevant to consider the free volume of glass. The free volume of a glass can be quantified by the atomic packing factor (APF) [75]. However, when plotting APF against the plastic compressibility for a variety of glass compositions, no relation is found (see appendix B).

That APF does not explain the resistance towards pressure densification indicates that it is the strength of the glass network, and not the available volume within it, which is the governing parameter. The strength of the glass network can be quantified from various approaches. When quantifying the strength of the glass network from elastic moduli or molar dissociation energy, no relation with plastic compressibility is found (see appendix C and appendix D). However, if using the dissociation energy per volume, instead of per mole, a correlation with the plastic compressibility is seen (cf. Figure 7-2). It is not surprising that a better trend is

found when scaling dissociation energy with volume, rather than moles, since volume is the metric of importance in relation to densification. However, a surprising finding is that the plastic compressibility increases with increasing dissociation energy. The cause of this is not understood, but one suggestion is that the types of networks formed with high dissociation energies favor a certain type of structural reorganization under pressure, facilitating densification. However, this requires further investigation.

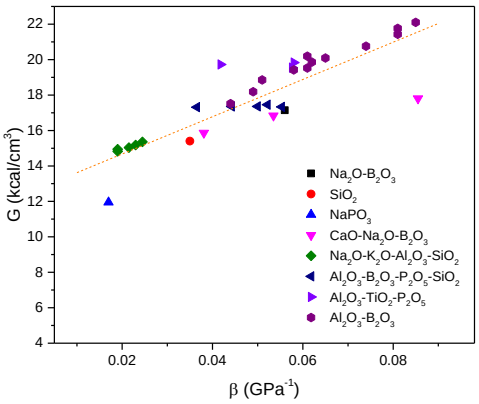

Figure 7-2. The dissociation energy per volume (G) plotted against the plastic compressibility (β) for a variety of glass compositions. G was calculated using data for dissociation energies from [73], by a similar protocol as described in appendix C for the molar dissociation energy. Plastic compressibility values were taken from: Na_2O-B_2O_3 [100], SiO_2 [100], $NaPO_3$ [72], CaO-Na_2O-B_2O_3 [24], Na_2O-K_2O-Al_2O_3-SiO_2 [31], Al_2O_3-B_2O_3-P_2O_5-SiO_2 [144], Al_2O_3-TiO_2-P_2O_5 [100], Al_2O_3-B_2O_3 [138]. The inserted line represents a least squares linear fit to the data (R^2=0.726) with intercept equal to 12.57 and slope equal to 105.17.

At high plastic compressibility, one borate glass shows large deviation from the trend line. This glass is very rich in B_2O_3 (85 mol%) [24] and is therefore expected to contain boroxol rings. The dissociation energies used from [73] are based on crystalline structures, and crystalline B_2O_3 does not contain boroxol rings. This might explain the discrepancy.

Another measure for the strength of the glass network is the hardness of glass. This is a measure of the resistance towards elasto-plastic deformation (from non-isostatic pressure). This may be used as an approximation to understand the resistance towards densification under hot isostatic pressure. However, when plotting hardness against plastic compressibility, no relation is found (see Figure 7-3).

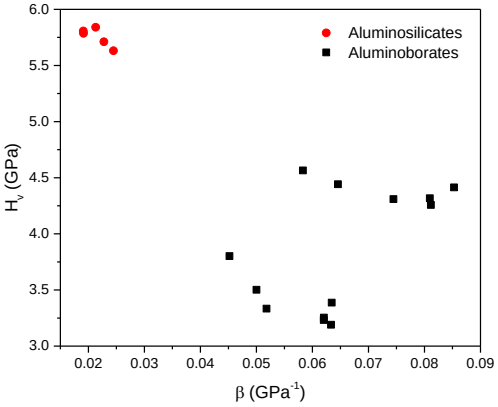

Figure 7-3. Hardness (H_v) and plastic compressibility (β) of selected glasses. Data for aluminosilicates taken from ref. [31], data for aluminoborates taken from ref. [138]. Hardness was measured at 1.94 N in all cases and plotted as the average value of 30 indents.

A deeper understanding of the glass hardness can be obtained from AFM measurements of indents using Yoshidas method [78]. This provides the volumes of densification and shear flow constituting the indentation imprint. The inset of Figure 7-4 shows the volumes of densification for the same glasses as plotted in Figure 7-3. Here no relation with plastic compressibility is found. The main figure shows the volume of shear flow plotted against the plastic compressibility of the same glasses. Interestingly, a relation between the volume of shear flow and plastic compressibility is seen. It should be noted that data for volumes of shear flow combined with plastic compressibility is only available for a limited number of glass compositions. Therefore, further test are required to validate the observed trend. The trend however indicates that densification during hot compression is related to shearing mechanisms.

It should be noted that investigations on the relations between plastic compressibility and properties above is based entirely on property measurement at ambient conditions. Various properties may change with increased pressure and temperature, and show other relations with the plastic compressibility under those conditions. E.g. densification during indentation may not scale with densification at elevated temperature, if the structural changes involved with the processes are very different. Pressure-densification at room temperature and at elevated temperature has e.g. previously been found to cause different structural changes [20][112].

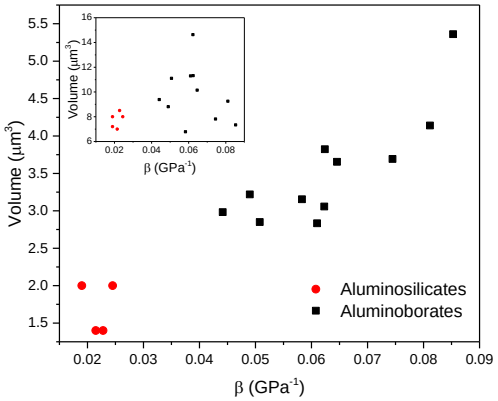

Figure 7-4. Volume of shear flow quantified from indentation imprints using Yoshidas method [78], plotted against the plastic compressibility (β), as determined after compression at T_g at 1 GPa. All indents were made using a load of 0.2 Kgf. Shear volumes represent the average of 10 indentations. Data for aluminoborates are taken from [138] and data for aluminosilicates is taken from [31]. Inset: Volume of densification plotted against the plastic compressibility (β).

7.2.1. SUMMARY

When investigating relations between changes in density and short- and intermediate range order after compression at T_g, it was found that these changes could not account for bulk density changes. Based on these results, we suggest that packing of structural units, as opposed to conversions between structural units, govern pressure-induced densification. We further suggest that changes in oxygen bond angles connecting network polyhedra are the main parameter governing pressure-densification. Changes in oxygen bond angels after hot compression has previously been found from ^{17}O MAS NMR of hot compressed glasses.

A relation between the dissociation energy per volume and the plastic compressibility was found. No explanation for the cause of this relation can be provided at present. One suggestion is however that glasses with higher dissociation energies per volume generally form a type of network which favors a type of structural reorganization under pressure, facilitating densification. In addition, a relation between the shear flow induced by indentation at ambient conditions and the plastic compressibility found after compression at T_g was also found. This indicates that densification resulting from hot compression is related to shearing mechanisms.

CHAPTER 8. GENERAL DISCUSSION

Compression causes marked changes in the structure of glass, including compaction of modifier environments, increased coordination number of network formers and a decrease in the fraction of intermediate range ring structures. Furthermore, compression causes an increase in hardness, enthalpy overshoot and density. The pressure-induced changes reach beyond those achievable by variations in composition and thermal history alone, and compression therefore offers an important means for exploration of structural regimes of glass.

As a method for property optimization, hot compression has proved efficient in increasing the hardness of glass. However, as we have also found [101], the hardness increase occurs with an accompanying decrease in crack resistance and increase in brittleness [24]. This is not desirable for most applications demanding high damage resistance, and the trade-off between improved hardness and diminished brittleness and crack resistance therefore poses a big issue in the use of compression for property optimization.

Compression has however shown a valuable tool as a method for the study on fundamental relations between structure-property and property-property relations in glass. E.g. relaxation experiments of hot compressed glasses offers a method for studying changes in structure-density-hardness relations for constant composition. A simple observation, such as the decoupling of relaxation times between hardness and density during relaxation, may have strong implications for our understanding on the structural origin of hardness. This type of experiment offers opportunities for structural studies throughout relaxation, enabling an unprecedented method for studies on variations in structure and properties for a constant composition.

The process of densification is an important part of forming an indentation imprint by indentation. Hereby, it is important to understand densification processes in order to understand the hardness of glass. Hardness and densification behavior in turn influence other mechanical properties, such as crack resistance [8]. The densification process induced by indentation may be approximated by studies on hot- or cold compression of bulk samples. Compression studies may therefore aid to understand the mechanical properties of glass (i.e. densification during indentation). No consensus on the pressure-induced structural changes governing densification has been achieved so far.

The pressure-induced structural changes governing density appear to be caused by changes in the backbone structure of the glass network, since increasing modifier content decreases the plastic compressibility [24]. As described in section Chapter 7, we suggest packing of structural units, as opposed to conversions between structural units, as the main parameter governing pressure-induced densification. We further

suggest that this packing of structural units is governed by changes in oxygen bond angles between network polyhedra. Such changes may be difficult to investigate unambiguously, though ^{17}O MAS NMR indicate these changes to occur in hot compressed glasses [37] [124][129] [130].

Based on a relation between the volume of shear flow induced by indentation, and the plastic compressibility resulting from hot compression (see Figure 7-4), we suggested the mechanisms governing densification to be related to shearing mechanisms. This relation between changes induced by indentation (shearing) and changes induced by hot compression (densification) also supports the idea of a relation between the structural changes induced by indentation under ambient conditions, and the structural changes resulting from hot compression. This principle is similar to a previous finding that the plastic compressibility resulting from hot compression scales with the extent of the indentation size effect, resulting from indentation under ambient conditions [145].

Various observations point towards specific structural changes governing the properties of hot compressed glasses. When comparing samples after ambient pressure sub-T_g annealing with hot compressed samples, and samples subjected to hot compression followed by relaxation, we find that similar changes in structure (e.g. BO_4 concentration, ring/non-ring BO_3) and properties (e.g. enthalpy overshoot, hardness) can be achieved across different densities, depending on the densification method applied. This indicates that these changes depend on specific structural features of the glass network. That the properties depend on specific structural features is also confirmed by our studies on the combined effects of hot compression and *in situ* (1 GPa) sub-T_g annealing (0.9 T_g). These two methods have been suggested to modify density and hardness through different structural mechanisms [114]. This is supported by our findings that hot compression (1 GPa, T_g) followed by *in situ* sub-T_g annealing (1 GPa, 0.9 T_g) caused changes in density, hardness and glass transition behavior, which cannot be achieved by sub-T_g annealing or hot compression alone. Hereby a novel route for design of structure and properties of glass is identified.

It remains a standing question whether full relaxation of pressure induced structural changes can be achieved by isothermal sub-T_g annealing (e.g. annealing at 0.9 T_g) at ambient pressure. It has previously been found that such treatment of hot compressed CaO-Na_2O-B_2O_3 glasses did not cause relaxation of pressure-induced BO_4 concentration [22]. We performed DSC scans, hardness and density measurements on the above described samples (hot compressed and *in situ* sub-T_g annealed) throughout relaxation. The results showed that full relaxation was obtained for these parameters after prolonged annealing at 0.9 T_g at ambient pressure. It is important to note that the glasses did not relax towards the prior uncompressed state, but rather towards the same state as an uncompressed glass relaxed under the same conditions (i.e. low T_f). DSC measurements allow for

analysis of changes in the glass transition behavior. It is interesting whether a relation between pressure-induced changes in thermodynamic properties and mechanical properties exist. However, it was found that while both the enthalpy overshoot and the hardness increased after compression, the hardness decreased while the enthalpy overshoot further increased during subsequent relaxation, i.e. no apparent relation between these parameters was found. A similar pattern was seen for density. This finding again points towards specific structural changes governing different properties of glass, and compression and relaxation experiments offers a potential means to identify these changes and study them throughout decoupled variations of each parameter.

Some interesting findings were made on general behaviors of glasses after hot compression. It was found that a general relation between the relative changes in density, elastic moduli and hardness applies for a variety of glass compositions. The structural basis of this relation was not identified, however, such relations potentially allow for predictive modelling of changes in properties of glasses outside of the compositional regimes investigated. Furthermore, a relation between the plastic compressibility and the dissociation energy per volume was found, across a wide range of glass compositions. Surprisingly, it was found that increasing dissociation energy caused an increased compressibility. We suggested this might be caused by networks of high dissociation energies forming network arrangements favoring densification under loading. This however remains to be investigated. This relation may provide a basis for predictive modelling of compressibilities for various glass compositions, knowing only the dissociation energies of the constituent oxide components. However, the dissociation energies of the oxide components is based on data for crystals, and it should therefore be noted that discrepancies between modeled and experimental results can be expected, where glass and crystal structure of oxide components show large deviations (e.g. B_2O_3). Densification during loading has previously been found to decrease crack formation and propagation [8]. The relation between dissociation energy per volume and plastic compressibility may therefore also have implications for designing glasses with high crack resistance.

LITERATURE LIST

[1] N. J. Kreidl, “Recent Applications of Glass Science,” *J. Non. Cryst. Solids*, vol. 123, pp. 377–384, 1990.

[2] C. R. Kurkjian and W. R. Prindle, “Perspectives on the History of Glass Composition,” *J. Am. Ceram. Soc.*, vol. 81, no. 4, pp. 795–813, 2005.

[3] A. Winkelmann and O. Schott, “Ueber die Elasticität und über die Zug- und Druckfestigheit vershiedener neuer Gläser in ihrer Abhängigkeit von der chemischen Zusammensetzung,” *Ann. Phys.*, vol. 287, no. 4, pp. 697–729, 1894.

[4] C. A. Angell, “Formation of Glasses from Liquids and Biopolymers,” *Science (80-.).*, vol. 267, no. 5206, pp. 1924–1935, 1995.

[5] S. Striepe, M. Potuzak, M. M. Smedskjaer, and J. Deubener, “Relaxation kinetics of the mechanical properties of an aluminosilicate glass,” *J. Non. Cryst. Solids*, vol. 362, no. 1, pp. 40–46, 2013.

[6] K. C. Lyon, “Prediction of the viscosities of ‘soda-lime’ silica glasses,” *J. Res. Natl. Bur. Stand. Sect. A Phys. Chem.*, vol. 78A, no. 4, p. 497, 1974.

[7] J. C. Mauro, Y. Yue, A. J. Ellison, P. K. Gupta, and D. C. Allan, “Viscosity of glass-forming liquids,” *Proc. Nat. Acad. Sci.*, vol. 106, p. 19780, 2009.

[8] J. C. Mauro, A. Tandia, K. D. Vargheese, Y. Z. Mauro, and M. M. Smedskjaer, “Accelerating the Design of Functional Glasses through Modeling,” *Chem. Mater.*, vol. 28, no. 12, pp. 4267–4277, 2016.

[9] G. N. Greaves and S. Sen, “Inorganic glasses, glass-forming liquids and amorphizing solids,” *Adv. Phys.*, vol. 56, no. 1, pp. 1–166, 2007.

[10] G. N. Greaves, “EXAFS and the structure of glass,” *J. Non. Cryst. Solids*, vol. 71, no. 1–3, pp. 203–217, 1985.

[11] G. N. Greaves, W. Smith, E. Giulotto, and E. Pantos, “Local structure, microstructure and glass properties,” *J. Non. Cryst. Solids*, vol. 222, pp. 13–24, 1997.

[12] M. M. Smedskjaer, J. C. Mauro, R. E. Youngman, C. L. Hogue, M. Potuzak, and Y. Yue, “Topological principles of borosilicate glass chemistry,” *J. Phys. Chem. B*, vol. 115, no. 44, pp. 12930–12946, 2011.

[13] J. D. Mackenzie, "High-pressure Effects on Oxide Glasses : I, Densification in Rigid State," *J. Am. Ceram. Soc.*, vol. 46, no. 10, pp. 461–470, 1963.

[14] J. D. Mackenzie, "High-pressure Effects on Oxide Glasses: III, Densification in Nonrigid State," *J. Am. Ceram. Soc.*, vol. 47, no. 2, pp. 76–80, 1964.

[15] J. D. Mackenzie, "High-pressure Effects on Oxide Glasses: II, Subsequent Heat Treatmanet," *J. Am. Ceram. Soc.*, vol. 46, no. 10, pp. 470–476, 1963.

[16] A. Zeidler, K. Wezka, D. A. J. Whittaker, P. S. Salmon, A. Baroni, S. Klotz, H. E. Fischer, M. C. Wilding, C. L. Bull, M. G. Tucker, M. Salanne, G. Ferlat, and M. Micoulaut, "Density-driven structural transformations in B_2O_3 glass," *Phys. Rev. B*, vol. 90, no. 2, p. 24206, 2014.

[17] A. C. Wright, C. E. Stone, R. N. Sinclair, N. Umesaki, N. Kitamura, K. Ura, N. Ohtori, and A. C. Hannon, "Structure of pressure compacted vitreous boron oxide," *Phys. Chem. Glas.*, vol. 41, no. 5, pp. 296–299, 2000.

[18] G. E. Gurr, P. W. Montgomery, C. D. Knutson, and B. T. Gorres, "The Crystal Structure of Trigonal Diboron Trioxide," *Acta Cryst. (1970).*, vol. B26, pp. 906–915, 1968.

[19] S. Maj, "On the relationship between refractive index and density for SiO_2 polymorphs," *Phys. Chem. Miner.*, vol. 16, no. 3, pp. 286–290, 1988.

[20] M. Guerette, M. R. Ackerson, J. Thomas, F. Yuan, E. B. Watson, D. Walker, and L. Huang, "Structure and properties of silica glass densified in cold compression and hot compression," *Sci. Rep.*, vol. 5, p. 15343, 2015.

[21] S. K. Lee, P. J. Eng, H. Mao, Y. Meng, M. Newville, M. Y. Hu, and J. Shu, "Probing of bonding changes in B2O3 glasses at high pressure with inelastic X-ray scattering," *Nat. Mater.*, vol. 4, no. 11, pp. 851–854, 2005.

[22] M. M. Smedskjaer, R. E. Youngman, S. Striepe, M. Potuzak, U. Bauer, J. Deubener, H. Behrens, J. C. Mauro, and Y. Yue, "Irreversibility of pressure induced boron speciation change in glass.," *Sci. Rep.*, vol. 4, p. 3770, 2014.

[23] S. Keun, J. Lin, Y. Q. Cai, N. Hiraoka, P. J. Eng, T. Okuchi, and H. Mao, "X-ray Raman scattering study of $MgSiO_3$ glass at high pressure : Implication for triclustered $MgSiO_3$ melt in Earth ' s mantle," *Proc. Natl. Acad. Sci.*, vol. 105, no. 23, 2008.

[24] S. Striepe, M. M. Smedskjaer, J. Deubener, U. Bauer, H. Behrens, M.

Potuzak, R. E. Youngman, J. C. Mauro, and Y. Yue, “Elastic and micromechanical properties of isostatically compressed soda-lime-borate glasses,” *J. Non. Cryst. Solids*, vol. 364, no. 1, pp. 44–52, 2013.

[25] L. Wondraczek, J. C. Mauro, J. Eckert, U. Kühn, J. Horbach, J. Deubener, and T. Rouxel, “Towards ultrastrong glasses,” *Adv. Mater.*, vol. 23, no. 39, pp. 4578–4586, 2011.

[26] E. W. Taylor, “Plastic deformation of optical glass,” *Nature*, vol. 163, no. 4139. p. 323, 1949.

[27] K. W. Peter, “Densification and flow phenomena of glass in indentation experiments,” *J. Non. Cryst. Solids*, vol. 5, pp. 130–115, 1970.

[28] J. T. Hagan, “Shear deformation under pyramidal indentations in soda-lime glass,” *J. Mater. Sci.*, vol. 15, no. 6, pp. 1417–1424, 1980.

[29] F. M. Ernsberger, “Mechanical Properties of Glass,” *J. Non. Cryst. Solids*, vol. 25, no. 1–3, pp. 293–321, 1977.

[30] M. M. Smedskjaer, S. J. Rzoska, M. Bockowski, and J. C. Mauro, “Mixed alkaline earth effect in the compressibility of aluminosilicate glasses,” *J. Chem. Phys.*, vol. 140, no. 5, 2014.

[31] K. G. Aakermann, K. Januchta, J. A. L. Pedersen, M. N. Svenson, S. J. Rzoska, M. Bockowski, J. C. Mauro, M. Guerette, L. Huang, and M. M. Smedskjaer, “Indentation deformation mechanism of isostatically compressed mixed alkali aluminosilicate glasses,” *J. Non. Cryst. Solids*, vol. 426, pp. 175–183, 2015.

[32] K. Hirao, Z. Zhang, H. Morita, and N. Soga, “Effect of Densification Treatment on the Mechanical Properties of Borate Glasses,” *J. Soc. Mater. Sci. Japan*, vol. 40, no. 451, pp. 400–404, 1990.

[33] S. K. Lee, “Microscopic origins of macroscopic properties of silicate melts and glasses at ambient and high pressure: Implications for melt generation and dynamics,” *Geochim. Cosmochim. Acta*, vol. 69, no. 14, pp. 3695–3710, 2005.

[34] B. T. Poe, P. F. Mcmillan, D. C. Rubie, S. Chakraborty, J. Yarger, and J. Diefenbacher, “Silicon and Oxygen Self-Diffusivities in Silicate Liquids Measured to 15 Gigapascals and 2800 Kelvin,” *Science (80-.).*, vol. 276, no. May, 1997.

[35] J. R. Allwardt, J. F. Stebbins, H. Terasaki, L. S. Du, D. J. Frost, A. C. Withers, M. M. Hirschmann, A. Suzuki, and E. Ohtani, "Effect of structural transitions on properties of high-pressure silicate melts:^{27}Al NMR, glass densities, and melt viscosities," *Am. Mineral.*, vol. 92, no. 7, pp. 1093–1104, 2007.

[36] S. J. Gaudio, C. E. Lesher, H. Maekawa, and S. Sen, "Linking high-pressure structure and density of albite liquid near the glass transition," *Geochim. Cosmochim. Acta 157*, vol. 157, pp. 28–38, 2015.

[37] S. K. Lee, "Structure of Silicate Glasses and Melts at High Pressure : Quantum Chemical Calculations and Solid-State NMR," pp. 5889–5900, 2004.

[38] D. T. Fearon, "Through the glass lightly," *Science (80-.).*, vol. 267, no. 5204, p. 1612, 1995.

[39] P. G. Debenedetti and F. H. Stillinger, "Supercooled liquids and the glass transition," *Nature*, vol. 410, no. 6825, p. 259, 2001.

[40] J. C. Mauro, D. C. Allan, and M. Potuzak, "Nonequilibrium viscosity of glass," *Phys. Rev. B - Condens. Matter Mater. Phys.*, vol. 80, no. 9, pp. 1–18, 2009.

[41] Y. Z. Yue, "Characteristic temperatures of enthalpy relaxation in glass," *J. Non. Cryst. Solids*, vol. 354, no. 12–13, pp. 1112–1118, 2008.

[42] Y. Yue, "The iso-structural viscosity, configurational entropy and fragility of oxide liquids," *J. Non. Cryst. Solids*, vol. 355, no. 10–12, pp. 737–744, 2009.

[43] X. Guo, M. Potuzak, J. C. Mauro, D. C. Allan, T. J. Kiczenski, and Y. Yue, "Unified approach for determining the enthalpic fictive temperature of glasses with arbitrary thermal history," *J. Non. Cryst. Solids*, vol. 357, no. 16–17, pp. 3230–3236, 2011.

[44] C. T. Moynihan, A. J. Easteal, M. A. DeBolt, and J. Tucker, "Dependence of the fictive temperture of glass on cooling rate," *J. Am. Ceram. Soc.*, vol. 59, no. 1–2, pp. 12–16, 1975.

[45] C. T. Moynihan, "Correlation between the Width of the Glass-Transition Region and the Temperature-Dependence of the Viscosity of High-T_g Glasses," *J. Am. Ceram. Soc.*, vol. 76, no. 5, pp. 1081–1087, 1993.

[46] Y. Yue, L. Wondraczek, H. Behrens, and J. Deubener, "Glass transition in an isostatically compressed calcium metaphosphate glass," *J. Chem. Phys.*, vol. 126, no. 14, 2007.

[47] L. Wondraczek, H. Behrens, Y. Yue, J. Deubener, and G. W. Scherer, "Relaxation and glass transition in an isostatically compressed diopside glass," *J. Am. Ceram. Soc.*, vol. 90, no. 5, pp. 1556–1561, 2007.

[48] L. Boehm, M. D. Ingram, and C. A. Angell, "Test of year-annealed glass for the Cogen-Grest percolation transition," *J. Non. Cryst. Solids*, vol. 44, pp. 305–313, 1981.

[49] B. Martin, L. Wondraczek, J. Deubener, and Y. Yue, "Mechanically induced excess enthalpy in inorganic glasses," *Appl. Phys. Lett.*, vol. 86, no. 12, pp. 1–3, 2005.

[50] X. Guo, "Glass Transition and Relaxation: Insights from Calorimetry," Aalborg University, 2012.

[51] W. H. Zachariasen, "The atomic arrangement in glass," *J. Am. Chem. Soc.*, vol. 54, no. 1, pp. 3841–3851, 1932.

[52] R. L. Mozzi and B. E. Warren, "The structure of vitreous boron oxide," *J. Appl. Crystallogr.*, vol. 3, no. 4, pp. 251–257, 1970.

[53] G. Ferlat, T. Charpentier, A. P. Seitsonen, A. Takada, M. Lazzeri, L. Cormier, G. Calas, and F. Mauri, "Boroxol rings in liquid and vitreous B_2O_3 from first principles," *Phys. Rev. Lett.*, vol. 101, no. 6, pp. 9–12, 2008.

[54] P. Y. Huang, S. Kurasch, A. Srivastava, V. Skakalova, J. Kotakoski, A. V. Krasheninnikov, R. Hovden, Q. Mao, J. C. Meyer, J. Smet, D. A. Muller, and U. Kaiser, "Direct imaging of a two-dimensional silica glass on graphene," *Nano Lett.*, vol. 12, no. 2, pp. 1081–1086, 2012.

[55] R. L. Mozzi and B. E. Warren, "The structure of vitreous silica," *J. Appl. Crystallogr.*, vol. 2, pp. 164–172, 1969.

[56] D. R. Neuville, L. Cormier, V. Montouillout, P. Florian, F. Millot, J. C. Rifflet, and D. Massiot, "Structure of Mg- and Mg/Ca aluminosilicate glasses: ^{27}Al NMR and Raman spectroscopy investigations," *Am. Mineral.*, vol. 93, no. 11–12, pp. 1721–1731, 2008.

[57] G. E. Jellison, L. W. Panek, P. J. Bray, and G. B. Rouse, "Determinations of structure and bonding in vitreous B_2O_3 by means of B^{10}, B^{11}, and O^{17}

NMR," *J. Chem. Phys.*, vol. 66, no. 2, pp. 802–812, 1977.

[58] A. C. Hannon, D. I. Grimley, R. A. Hulme, A. C. Wright, and R. N. Sinclair, "Boroxol groups in vitreous boron oxide: new evidence from neutron diffraction and inelastic neutron scattering studies," *J. Non. Cryst. Solids*, vol. 177, pp. 299–316, 1994.

[59] J. E. Shelby, "Thermal Expansion of Alkali Borate Glasses," *J. Am. Ceram. Soc.*, vol. 66, no. 3, pp. 225–227, 1982.

[60] J. Zhong and P. J. Bray, "Change in Boron Coordination in Alkali Borate Glasses, and Mixed Alkali Effects, as Elucidated by NMR," *J. Non. Cryst. Solids*, vol. 111, pp. 67–76, 1989.

[61] S. Wang and J. Stebbins, "On the structure of borosilicate glasses: a triple-quantum magic-angle spinning ^{17}O nuclear magnetic resonance study," *J. Non. Cryst. Solids*, vol. 231, no. 3, pp. 286–290, 1998.

[62] S. K. Lee and J. F. Stebbins, "Extent of intermixing among framework units in silicate glasses and melts," *Geochim. Cosmochim. Acta*, vol. 66, no. 2, pp. 303–309, 2002.

[63] L.-S. Du and J. F. Stebbins, "Nature of Silicon-Boron Mixing in Sodium Borosilicate Glasses: A High-Resolution ^{11}B and ^{17}O NMR Study," *J. Non. Cryst. Solids*, vol. 107, no. 9, pp. 10063–10076, 2003.

[64] R. K. Brow, C. A. Click, and T. M. Alam, "Modifier coordination and phosphate glass networks," *J. Non-Cryst. Solids*, vol. 274, pp. 9–16, 2000.

[65] T. Grande, J. R. Holloway, P. F. McMillan, and C. A. Angell, "Nitride glasses obtained by high-pressure synthesis," *Nature*, vol. 367, no. 6463, pp. 532–8, 1994.

[66] T. Grande, S. Jacob, J. R. Holloway, P. F. McMillan, and C. A. Angell, "High-pressure synthesis of nitride glasses," *J. Non. Cryst. Solids*, vol. 184, no. 1, pp. 151–154, 1995.

[67] F. Munoz, A. Duran, L. Pascual, and R. Marchand, "Compositional and viscosity influence on the nitrogen/oxygen substitution reactions in phosphate melts," *Phys. Chem. Glas.*, vol. 46, no. 1, pp. 39–45, 2005.

[68] A. Le Sauze, L. Montagne, G. Palavit, F. Fayon, and R. Marchand, "X-ray photoelectron spectroscopy and nuclear magnetic resonance structural study of phosphorus oxynitride glasses, 'LiNaPON,'" *J. Non. Cryst. Solids*, vol.

263–264, pp. 139–145, 2000.

[69] S. Hampshire and M. J. Pomeroy, “Oxynitride glasses,” *Int. J. Appl. Ceram. Technol.*, vol. 5, no. 2, pp. 155–163, 2008.

[70] P. F. Becher, S. Hampshire, M. J. Pomeroy, M. J. Hoffmann, M. J. Lance, and R. L. Satet, “An Overview of the Structure and Properties of Silicon-Based Oxynitride Glasses,” *Int. J. Appl. Glas. Sci.*, vol. 2, no. 1, pp. 63–83, 2011.

[71] S. Hampshire, “Oxynitride glasses, their properties and crystallisation - A review,” *J. Non. Cryst. Solids*, vol. 316, no. 1, pp. 64–73, 2003.

[72] M. N. Svenson, L. G. Paraschiv, F. Munoz, Y. Yue, S. J. Rzoska, M. Bockowski, and L. R. Jensen, “Pressure-Induced Structural Transformations in Phosphorus Oxynitride Glasses,” *J. Non. Cryst. Solids*, vol. 52, pp. 153–160, 2016.

[73] A. Makishima and J. D. Mackenzie, “Direct calculation of Young’s modulus of glass,” *J. Non. Cryst. Solids*, vol. 12, no. 1, pp. 35–45, 1973.

[74] G. A. Rosales-Sosa, A. Masuno, Y. Higo, H. Inoue, Y. Yanaba, T. Mizoguchi, T. Umada, K. Okamura, K. Kato, and Y. Watanabe, “High Elastic Moduli of a $54Al_2O_3$-$46Ta_2O_5$ Glass Fabricated via Containerless Processing.,” *Sci. Rep.*, vol. 5, p. 15233, 2015.

[75] T. Rouxel, “Elastic properties and short-to medium-range order in glasses,” *J. Am. Ceram. Soc.*, vol. 90, no. 10, pp. 3019–3039, 2007.

[76] M. Yamane and J. D. Mackenzie, “Vicker’s Hardness of glass,” *J. Non. Cryst. Solids*, vol. 15, no. 2, pp. 153–164, 1974.

[77] M. Smedskjaer, J. Mauro, and Y. Yue, “Prediction of Glass Hardness Using Temperature-Dependent Constraint Theory,” *Phys. Rev. Lett.*, vol. 105, no. 11, pp. 10–13, 2010.

[78] S. Yoshida, J.-C. Sanglebœuf, and T. Rouxel, “Quantitative evaluation of indentation-induced densification in glass,” *J. Mater. Res.*, vol. 20, no. 12, pp. 3404–3412, 2005.

[79] S. Striepe, J. Deubener, M. Potuzak, M. M. Smedskjaer, and A. Matthias, “Thermal history dependence of indentation induced densification in an aluminosilicate glass,” *J. Non. Cryst. Solids*, vol. 445, pp. 34–39, 2016.

[80] S. K. Lee, P. J. Eng, H. K. Mao, and J. Shu, "Probing and modeling of pressure-induced coordination transformation in borate glasses: Inelastic x-ray scattering study at high pressure," *Phys. Rev. B - Condens. Matter Mater. Phys.*, vol. 78, no. 21, pp. 30–35, 2008.

[81] S. Buchner, A. S. Pereira, J. C. De Lima, and N. M. Balzaretti, "X-ray study of lithium disilicate glass: High pressure densification and polyamorphism," *J. Non. Cryst. Solids*, vol. 387, pp. 112–116, 2014.

[82] J. Nicholas, S. Sinogeikin, J. Kieffer, and J. Bass, "Spectroscopic Evidence of Polymorphism in Vitreous B_2O_3," *Phys. Rev. Lett.*, vol. 92, no. 21, p. 215701, 2004.

[83] C. Meade, R. J. Hemley, and H. K. Mao, "High-Pressure X-Ray Diffraction of $Si0_2$ Glass," *Physcial Rev. Lett.*, vol. 69, no. 9, pp. 1387–1391, 1992.

[84] C. J. Benmore, E. Soignard, S. A. Amin, M. Guthrie, S. D. Shastri, P. L. Lee, and J. L. Yarger, "Structural and topological changes in silica glass at pressure," *Phys. Rev. B - Condens. Matter Mater. Phys.*, vol. 81, no. 5, pp. 1–5, 2010.

[85] S. Susman, K. J. Volin, D. L. Price, M. Grimsditch, J. P. Rino, R. K. Kalia, and P. Vahishta, "Intermediate range order in permanently densified vitreous SiO_2: A neutron-diffraction and molecular dynamics study," *Phys. Rev. B - Condens. Matter Mater. Phys.*, vol. 43, no. 1, pp. 1194–1197, 1991.

[86] F. L. galeener, A. J. Leadbetter, and M. W. Stringfellow, "Comparison of the neutron, Raman, and infrared vibrational spectra of vitreous $Si0_2$, GeO_2, and BeF_2," *Phys. Rev. B - Condens. Matter Mater. Phys.*, vol. 27, no. 2, pp. 1052–1078, 1983.

[87] A. Jayaraman, "Diamond anvil cell and high-pressure physical investigations," *Rev. Mod. Phys.*, vol. 55, no. 1, pp. 65–108, 1983.

[88] M. Kanzak, "Melting of Silica up to 7 GPa," *J Am Cerom Soc*, vol. 73, no. 12, pp. 3706–3707, 1990.

[89] B. T. Poe, C. Romano, and G. Henderson, "Raman and XANES spectroscopy of permanently densified vitreous silica," *J. Non. Cryst. Solids*, vol. 341, no. 1–3, pp. 162–169, 2004.

[90] T. Champagnon, J. Deschamps, C. Margueritat, A. Martinet, and B. Mermet, "Elastic moduli of permanently densified silica glasses," *Sci. Rep.*, vol. 4, p. 7193, 2014.

[91] D. Uhlmann, “Densification of alkali silicate glasses at high pressure,” *J. Non-Cryst. Solids*, vol. 13, pp. 89–99, 1973.

[92] P. Salmon and A. Zeidler, “Networks under pressure: the development of in situ highpressure neutron diffraction for glassy and liquid materials,” *J. Phys. Condens. Matter*, vol. 27, p. 133201, 2015.

[93] M. B. Østergaard, R. E. Youngman, M. N. Svenson, S. J. Rzoska, M. Bockowski, L. R. Jensen, and M. M. Smedskjaer, “Temperature-dependent densification of sodium borosilicate glass,” *RSC Adv.*, vol. 5, pp. 78845–78851, 2015.

[94] V. V. Brazhkin, I. Farnan, K. I. Funakoshi, M. Kanzaki, Y. Katayama, A. G. Lyapin, and H. Saitoh, “Structural transformations and anomalous viscosity in the B_2O_3 melt under high pressure,” *Phys. Rev. Lett.*, vol. 105, no. 11, pp. 1–4, 2010.

[95] J. Wu, J. Deubener, J. F. Stebbins, L. Grygarova, H. Behrens, L. Wondraczek, and Y. Yue, “Structural response of a highly viscous aluminoborosilicate melt to isotropic and anisotropic compressions,” *J. Chem. Phys.*, vol. 131, no. 10, pp. 1–10, 2009.

[96] S. Bista, J. F. Stebbins, W. B. Hankins, and T. W. Sisson, “Aluminosilicate melts and glasses at 1 to 3 GPa: Temperature and pressure effects on recovered structural and density changes,” *Am. Mineral.*, vol. 100, no. 10, pp. 2298–2307, 2015.

[97] N. S. Bagdassarov, J. Maumus, B. Poe, A. B. Slutskiy, and V. K. Bulatov, “Pressure dependence of T g in silicate glasses from electrical impedance measurements,” *Phys. Chem. Glas. - Eur. J. Glas. Sci. Technol. Part B*, vol. 45, no. 3, pp. 197–214, 2004.

[98] A. Drozd-Rzoska, S. J. Rzoska, M. Paluch, A. R. Imre, and C. M. Roland, “On the glass temperature under extreme pressures,” *J. Chem. Phys.*, vol. 126, no. 16, pp. 1–7, 2007.

[99] T. Sato, N. Funamori, and T. Yagi, “Helium penetrates into silica glass and reduces its compressibility.,” *Nat. Commun.*, vol. 2, no. May, p. 345, 2011.

[100] M. N. Svenson, M. Guerette, L. Huang, N. Lönnroth, J. C. Mauro, S. J. Rzoska, M. Bockowski, and M. M. Smedskjaer, “Universal behavior of changes in elastic moduli of hot compressed oxide glasses,” *Chem. Phys. Lett.*, vol. 651, pp. 88–91, 2016.

[101] M. N. Svenson, T. K. Bechgaard, S. D. Fuglsang, R. H. Pedersen, A. O. Tjell, M. B. ??stergaard, R. E. Youngman, J. C. Mauro, S. J. Rzoska, M. Bockowski, and M. M. Smedskjaer, "Composition-Structure-Property Relations of Compressed Borosilicate Glasses," *Phys. Rev. Appl.*, vol. 2, no. 2, pp. 1–9, 2014.

[102] M. N. Svenson, L. M. Thirion, R. E. Youngman, J. C. Mauro, S. J. Rzoska, M. Bockowski, and M. M. Smedskjaer, "Pressure-induced changes in interdiffusivity and compressive stress in chemically strengthened glass," *ACS Appl. Mater. Interfaces*, vol. 6, no. 13, pp. 10436–10444, 2014.

[103] M. N. Svenson, L. M. Thirion, R. E. Youngman, J. C. Mauro, M. Bauchy, S. J. Rzoska, M. Bockowski, and M. M. Smedskjaer, "Effects of Thermal and Pressure Histories on the Chemical Strengthening of Sodium Aluminosilicate Glass," *Front. Mater.*, vol. 3, no. March, pp. 1–11, 2016.

[104] M. N. Svenson, R. E. Youngman, Y. Yue, S. J. Rzoska, M. Bockowski, L. R. Jensen, and M. M. Smedskjaer, "Volume and Structure Relaxation in Compressed Sodium Borate Glass," *Submitt. to PCCP*, 2016.

[105] M. N. Svenson, J. C. Mauro, S. J. Rzoska, M. Bockowski, and M. M. Smedskjaer, "Accessing Forbidden Glass Regimes through High-Pressure Sub-T_g Annealing," *To be Submitt.*, 2016.

[106] C. . A. Angell, K. L. Ngai, G. B. McKenna, P. F. McMillan, and S. W. Martin, "Relaxation in glassforming liquids and amorphous solids," *J. Appl. Phys.*, vol. 88, no. 6, p. 3113, 2000.

[107] A. Q. Tool, "Relation Between Inelastic Deformability and Thermal Expansion of Glass in Its Annealing Range," *J. Am. Ceram. Soc.*, vol. 29, no. 9, pp. 240–253, 1946.

[108] R. Kolsrauch, "Theorie des elektrischen Rückstandes in der Leidener Flasche," *Ann. Phys.*, vol. 167, no. 2, pp. 179–214, 1854.

[109] J. C. Phillips, "Stretched exponential relaxation in molecular and electronic glasses," *rep. prog. phys.*, vol. 59, pp. 1133–1207, 1996.

[110] M. N. Svenson, M. Guerette, L. Huang, and M. M. Smedskjaer, "Raman spectroscopy study of pressure-induced structural changes in sodium borate glass," *J. Non. Cryst. Solids*, vol. 443, pp. 130–135, 2016.

[111] T. Edwards, T. Endo, J. H. Walton, and S. Sen, "Observation of the transition state for pressure-induced $BO_3 \rightarrow BO_4$ conversion in glass,"

Science (80-.)., vol. 345, no. 6200, pp. 1027–1029, 2014.

[112] L. Wondraczek, S. Sen, H. Behrens, and R. E. Youngman, "Structure-energy map of alkali borosilicate glasses: Effects of pressure and temperature," *Phys. Rev. B - Condens. Matter Mater. Phys.*, vol. 76, no. 1, pp. 1–8, 2007.

[113] J. R. Allwardt, J. F. Stebbins, B. C. Schmidt, D. J. Frost, A. C. Withers, and M. M. Hirschmann, "Aluminum coordination and the densification of high-pressure aluminosilicate glasses," *Am. Mineral.*, vol. 90, no. 7, pp. 1218–1222, 2005.

[114] M. M. Smedskjaer, M. Bauchy, J. C. Mauro, S. J. Rzoska, and M. Bockowski, "Unique effects of thermal and pressure histories on glass hardness: Structural and topological origin," *J. Chem. Phys.*, vol. 143, no. 16, 2015.

[115] G. M, L. Huang, J. Nicholas, J. Kieffer, and J. Bass, "Irreversible structural changes in vitreous B2O3 under pressure," vol. 20, no. 1, pp. 152–155, 2008.

[116] S. K. Lee, K. Mibe, Y. Fei, G. D. Cody, and B. O. Mysen, "Structure of B_2O_3 glass at high pressure: A ^{11}B solid-state NMR study," *Phys. Rev. Lett.*, vol. 94, no. 16, pp. 27–30, 2005.

[117] J. Felten, H. Hall, J. Jaumot, R. Tauler, A. de Juan, and A. Gorzsás, "Vibrational spectroscopic image analysis of biological material using multivariate curve resolution–alternating least squares (MCR-ALS)," *Nat. Protoc.*, vol. 10, no. 2, pp. 217–240, 2015.

[118] B. N. Meera and J. Ramakrishna, "'Raman spectral studies of borate glasses,'" *J. Non-Cryst. Solids*, vol. 159, p. 1, 1993.

[119] W. L. L. Konijnendijk and J. M. M. Stevels, "The structure of borate glasses studied by Raman scattering," *J. Non. Cryst. Solids*, vol. 18, no. 3, pp. 307–331, 1975.

[120] C. F. Windisch and W. M. Risen, "Vibrational spectra of oxygen- and boron-isotopically substituted B_2O_3 glasses," *J. Non. Cryst. Solids*, vol. 48, no. 2–3, pp. 307–323, 1982.

[121] G. E. Walrafen, S. R. Samanta, and P. N. Krishnan, "Raman investigation of vitreous and molten boric oxide," *J. Chem. Phys.*, vol. 72, no. 1, pp. 113–120, 1980.

[122] S. K. Sharma, B. Simons, and J. F. M. 3, "Relationship Between Density, Refractive Index and Sstructure of B_2O_3 glasses at low and high pressures," *J. Non. Cryst. Solids*, vol. 42, no. 9, pp. 607–618, 1980.

[123] J. D. Nicholas, R. E. Youngman, S. V. Sinogeikin, J. D. Bass, and J. Kieffer, "Structural changes in vitreous boron oxide," *Phys. Chem. Glas.*, vol. 44, no. 3, pp. 249–251, 2003.

[124] S. K. Lee, G. D. Cody, Y. Fei, and B. O. Mysen, "Nature of polymerization and properties of silicate melts and glasses at high pressure," *Geochim. Cosmochim. Acta*, vol. 68, no. 20, pp. 4189–4200, 2004.

[125] K. E. Kelsey, J. F. Stebbins, J. L. Mosenfelder, and P. D. Asimow, "Simultaneous aluminum, silicon, and sodium coordination changes in 6 GPa sodium aluminosilicate glasses," *Am. Mineral.*, vol. 94, no. 8–9, pp. 1205–1215, 2009.

[126] X. Xue, J. F. Stebbins, M. Kanzaki, and R. G. Trønnes, "Silicon coordination and speciation changes in a silicate liquid at high pressures.," *Science*, vol. 245, no. 4921, pp. 962–4, 1989.

[127] Xianyu Xue, J. F. Stebbins, M. Kanzaki, P. F. McMillan, and B. Poe, "Pressure-induced silicon coordination and tetrahedral structural changes in alkali oxide-silica melts up to 12 GPa: NMR, Raman, and infrared spectroscopy," *Am. Mineral.*, vol. 76, no. 1–2, pp. 8–26, 1991.

[128] J. L. Yarger, K. H. Smith, R. A. Nieman, J. Diefenbacher, G. H. Wolf, B. T. Poe, and P. F. McMillan, "Al Coordination Changes in High-Pressure Aluminosilicate Liquids," *Science (80-.).*, vol. 270, no. 5244, pp. 1964–1967, 1995.

[129] S. K. Lee, Y. Fei, G. D. Cody, and B. O. Mysen, "Order and disorder in sodium silicate glasses and melts at 10 GPa," *Geophys. Res. Lett.*, vol. 30, no. 16, p. 1845, 2003.

[130] J. R. Allwardt, B. C. Schmidt, and J. F. Stebbins, "Structural mechanisms of compression and decompression in high-pressure $K_2Si_4O_9$ glasses: An investigation utilizing Raman and NMR spectroscopy of glasses and crystalline materials," *Chem. Geol.*, vol. 213, no. 1–3, pp. 137–151, 2004.

[131] L. S. Du, J. R. Allwardt, B. C. Schmidt, and J. F. Stebbins, "Pressure-induced structural changes in a borosilicate glass-forming liquid: Boron coordination, non-bridging oxygens, and network ordering," *J. Non. Cryst. Solids*, vol. 337, no. 2, pp. 196–200, 2004.

[132] M. Wilding, M. Guthrie, S. Kohara, C. L. Bull, J. Akola, and M. G. Tucker, "The structure of MgO-SiO_2 glasses at elevated pressure.," *J. Phys. Condens. Matter*, vol. 24, no. 22, p. 225403, 2012.

[133] X. Xue and J. F. Stebbins, "^{23}Na NMR chemical shifts and local Na coordination environments in silicate crystals, melts and glasses," *Phys. Chem. Miner.*, vol. 20, no. 5, pp. 297–307, 1993.

[134] A. M. George, S. Sen, and J. F. Stebbins, "^{23}Na chemical shifts and local structure in crystalline, glassy, and molten sodium borates and germanates.," *Solid State Nucl. Magn. Reson.*, vol. 10, no. 1–2, pp. 9–17, 1997.

[135] F. Muñoz, L. Delevoye, L. Montagne, and T. Charpentier, "New insights into the structure of oxynitride NaPON phosphate glasses by 17-oxygen NMR," *J. Non. Cryst. Solids*, vol. 363, no. 1, pp. 134–139, 2013.

[136] S. K. Lee, P. J. Eng, H. K. Mao, Y. Meng, and J. Shu, "Structure of alkali borate glasses at high pressure: B and Li K-edge inelastic X-ray scattering study," *Phys. Rev. Lett.*, vol. 98, no. 10, pp. 1–4, 2007.

[137] R. J. Hand and D. R. Tadjiev, "Mechanical properties of silicate glasses as a function of composition," *J. Non. Cryst. Solids*, vol. 356, no. 44–49, pp. 2417–2423, 2010.

[138] K. Januchta and M. Smedskjær, "Unpublished."

[139] A. Tandia, K. D. Vargheese, and J. C. Mauro, "Elasticity of ion stuffing in chemically strengthened glass," *J. Non. Cryst. Solids*, vol. 358, no. 12–13, pp. 1569–1574, 2012.

[140] R. J. Charles, "Structural State and Diffusion in a Silicate Glass," *J. Am. Ceram. Soc.*, vol. 45, no. 3, pp. 105–113, 1962.

[141] R. A. B. . Devine, "Si-0 bond-length modification in pressure-densified amorphous $Si0_2$," *Phys. Rev. B*, vol. 35, no. 17, pp. 9376–9379, 1987.

[142] M. Svenson, J. Mauro, S. J. Rzoska, M. Bockowski, and M. Smedskjær, "Unpublished."

[143] N. Lönroth, B. Atkins, M. Svenson, S. J. Rzoska, M. Bockowski, and M. Smedskjær, "Unpublished."

[144] S. Kapoor, X. Guo, R. E. Youngman, J. C. Mauro, S. J. Rzoska, and M. M. Smedskjær, "In preparation," 2016.

[145] M. M. Smedskjaer, "Indentation size effect and the plastic compressibility of glass," *Appl. Phys. Lett.*, vol. 104, no. 25, p. 251906, 2014.

[146] R. D. Shannon, "Revised Effective Ionic Radii and Systematic Studies of Interatomic Distances in Halides and Chaleogenides," *Acta Cryst.*, vol. A32, p. 751, 1976.

Appendix A. Chemical shift and quadropolar coupling constant

The isotropic chemical shift (δ_{CS}) and quadropolar coupling product (P_q) was calculated from the centers of gravity in the MAS (δ_2^{CG}) and isotropic dimensions (δ_{iso}^{CG}) accordin to the formulas below:

$$\delta_{CS} = \frac{10}{27}\delta_2^{CG} + \frac{17}{27}\delta_{iso}^{CG}$$

$$P_q = (\delta_{iso}^{CG} - \delta_2^{CG})^{1/2}\, f(s) v_0 \times 10^{-3}$$

Where F(S) is a constant, i.e. f(S) = 10.244 for spin-5/2 nuclei (^{27}Al) or 5.122 for spin-3/2 nuclei (^{23}Na). ν_0 is the resonance frequency of the quadrupolar nucleus in megahertz (MHz). P_q can be related to the quadrupolar coupling constant (C_q) as $P_q = C_q(1 + \eta_q^2/3)^{1/2}$, where η_q is the quadrupolar coupling asymmetry parameter.

Appendix B. Atomic Packing Factor

The free volume of a glass network can be quantified by calculating the atomic packing factor (APF) [75]. This parameter gives the ratio between the minimum theoretical volume occupied by one mole of the ions in the glass and the experimentally determined molar volume:

$$APF = \rho \frac{\sum f_i V_i}{\sum f_i M_i}$$

Where f_i is the molar fraction and M_i is the molar mass of the ith A_xB_y constituent (e.g. Al_2O_3), and $V_i = (4/3)\pi Na(x_{rA}^3 + y_{rB}^3)$ is the theoretical volume of the ions, with r_A being radius of the cation (e.g. Al) and r_B being the radius of the anion (e.g. O) and Na is Avogadro's number. Values for ionic radii can be found in the work of Shannon [146].

When calculating APF and plotting it against the plastic compressibility, no apparent relation is found (see Figure 8-1).

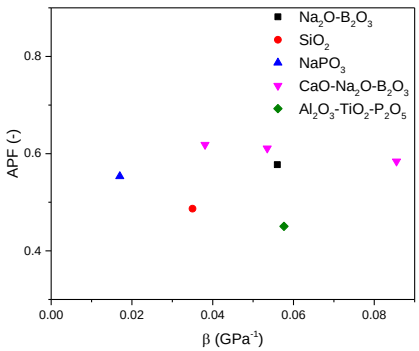

Figure 8-1. Atomic packing factor (APF) of selected glasses plotted against their plastic compressibility (β). Data taken from; Na_2O-B_2O_3 [104], $NaPO_4$ [72], SiO_2 [100], CaO-Na_2O-B_2O_3 [24], Al_2O_3-TiO_2-P_2O_5 [100].

It should however be noted that calculations of APF are only a theoretical approximation, since estimates of the ionic radii are based on crystalline configurations, and the effective ionic radii in glasses are not known with high accuracy [75].

Appendix C. Dissociation Energy

The molar dissociation energy of each glass was calculated from the molar fractions of the constituent oxide components. The dissociation energy of each oxide component was taken from [73].

$$U' = \sum f_i U'_i$$

Where f_i is the molar fraction of the constituent oxide and U'_i is the dissociation energy (kcal/mole).

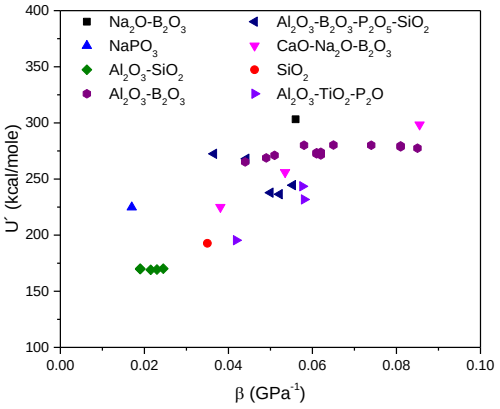

Figure 8-2. The molar dissociation energy (U´) of various oxide glasses plotted as a function of their plastic compressibility (β). Data included from: Na_2O-B_2O_3 [104], Al_2O_3-B_2O_3-P_2O_5-SiO_2 [144], $NaPO_3$ [72], CaO-Na_2O-B_2O_3 [24]. Al_2O_3-SiO_2 [31], SiO_2 [100], Al_2O_3-B_2O_3 [138], Al_2O_3-B_2O_3-P_2O_5-SiO_2 [144], Al_2O_3-TiO_2-P_2O_5 [100].

From the figure it may seem that a rough correlation between the molar dissociation energy and the plastic compressibility can be seen. However, upon further inspection, e.g. the Al_2O_3-B_2O_3 glasses or the Al_2O_3-B_2O_3-P_2O_5-SiO_2 glasses show a very poor correlation with the plastic compressibility.

Appendix D. Young modulus

Figure 8-3 shows Youngs modulus of various oxide glass compositions as determined by Brillouin spectroscopy, plotted against their plastic compressiblity. No apparent relation between Youngs modulus and the plastic compressibility is seen from the figure. No relation was found when plotting shear modulus or bulk modulus against the plastic compressibility either (not shown).

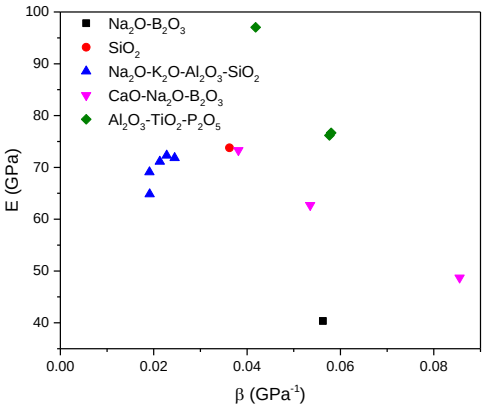

Figure 8-3. Youngs modulus (E) of various oxide glass compositions plotted against their plastic compressibility (β), as determined from compression at T_g. Data taken from [100].

ISSN (online): 2246-1248
ISBN (online): 978-87-7112-807-9

AALBORG UNIVERSITY PRESS